

Strength of jointed rock masses

Evert Hoek, Golder Associates, Vancouver, Canada

Twenty-third Rankine Lecture
presented to the British Geological Society in London on February 23, 1983
and published in *Géotechnique*, Vol. 23, No. 3, 1983, pp. 187-223.

Strength of jointed rock masses

Evert Hoek, Golder Associates, Vancouver, Canada

Synopsis

Jointed rock masses comprise interlocking angular particles or blocks of hard brittle material separated by discontinuity surfaces which may or may not be coated with weaker materials. The strength of such rock masses depends on the strength of the intact pieces and on their freedom of movement which, in turn, depends on the number, orientation, spacing and shear strength of the discontinuities. A complete understanding of this problem presents formidable theoretical and experimental problems and, hence, simplifying assumptions are required in order to provide a reasonable basis for estimating the strength of jointed rock masses for engineering design purposes. This paper summarizes some of the basic information upon which such simplifying assumptions can be made. A simple empirical failure criterion is presented and its application in engineering design is illustrated by means of a number of practical examples.

Introduction

The past twenty years have seen remarkable developments in the field of geotechnical engineering, particularly in the application of computers to the analysis of complex stress distribution and stability problems. There have also been advances in the field of geotechnical equipment and instrumentation and in the understanding of concepts such as the interaction between a concrete or steel structure and the soil foundation upon which it is built or, in the case of a tunnel, the interaction between the rock mass surrounding the tunnel and the support system installed in the tunnel. Similarly, there have been significant advances in our ability to understand and to analyze the role of structural features such as joints, bedding planes and faults in controlling the stability of both surface and underground excavations.

In spite of these impressive advances, the geotechnical engineer is still faced with some areas of major uncertainty and one of these relates to the strength of jointed rock masses. This problem is summed up very well in a paper on rockfill materials by Marachi, Chan and Seed (1972) when they say 'No stability analysis, regardless of how intricate and theoretically exact it may be, can be useful for design if an incorrect estimation of the shearing strength of the construction material has been made'. These authors go on to show that, although laboratory tests on rockfill are difficult and expensive because of the size of the equipment involved, there are techniques available to permit realistic and reliable evaluation of the shear strength of typical rockfill used for dam construction.

Unfortunately, this is not true for jointed rock masses where a realistic evaluation of shear strength presents formidable theoretical and experimental problems. However, since this question is of fundamental importance in almost all major designs involving foundations, slopes or underground excavations in rock, it is essential that such strength estimates be made and that these estimates should be as reliable as possible.

In this paper the author has attempted to summarize what is known about the strength of jointed rock masses, to deal with some of the theoretical concepts involved and to explore their limitations and to propose some simple empirical approaches which have been found useful in solving real engineering problems. Examples of such engineering problems are given.

Definition of the problem

Figure 1 summarises the range of problems to be considered. In order to understand the behaviour of jointed rock masses, it is necessary to start with the components which go together to make up the system - the intact rock material and individual discontinuity surfaces. Depending upon the number, orientation and nature of the discontinuities, the intact rock pieces will translate, rotate or crush in response to stresses imposed upon the rock mass. Since there are a large number of possible combinations of block shapes and sizes, it is obviously necessary to find any behavioural trends which are common to all of these combinations. The establishment of such common trends is the most important objective of this paper.

Before embarking upon a study of the individual components and of the system as a whole, it is necessary to set down some basic definitions.

Intact rock refers to the unfractured blocks which occur between structural discontinuities in a typical rock mass. These pieces may range from a few millimetres to several metres in size and their behaviour is generally elastic and isotropic. Their failure can be classified as brittle which implies a sudden reduction in strength when a limiting stress level is exceeded. In general, viscoelastic or time-dependent behaviour such as creep is not considered to be significant unless one is dealing with evaporites such as salt or potash.

Joints are a particular type of geological discontinuity but the term tends to be used generically in rock mechanics and it usually covers all types of structural weakness. Strength, in the context of these notes, refers to the maximum stress level which can be carried by a specimen. No attempt is made to relate this strength to the amount of strain which the specimen undergoes before failure nor is consideration given to the post-peak behaviour or the relationship between peak and residual strength. It is recognised that these factors are important in certain engineering applications but such problems are beyond the scope of this paper.

The presentation of rock strength data and its incorporation into a failure criterion depends upon the preference of the individual and upon the end use for which the criterion is intended. In dealing with slope stability problems where limit equilibrium methods of analyses are used, the most useful failure criterion is one which expresses the shear strength in terms of the effective normal stress acting across a particular weakness plane or shear zone. The presentation which is most familiar to soil mechanics engineers is the Mohr failure envelope. On the other hand, when analysing the stability of underground excavations, the response of the rock to the principal stresses acting upon each element is of paramount interest. Consequently, a plot of triaxial test data in terms of the major principal stress at failure versus minimum principal stress or confining pressure is the most useful form of failure criterion for

the underground excavation engineer. Other forms of failure criterion involving induced tensile strain, octahedral shear stress or energy considerations will not be dealt with.

In recognition of the soil mechanics background of many of the readers, most of the discussion on failure criteria will be presented in terms of Mohr failure envelopes. It is, however, necessary to point out that the author's background in underground excavation engineering means that the starting point for most of his studies is the triaxial test and the presentation of failure criteria in terms of principal stresses rather than shear and normal stresses. As will become obvious later, this starting point has an important bearing upon the form of the empirical failure criterion presented here.

Strength of intact rock

A vast amount of information on the strength of intact rock has been published during the past fifty years and it would be inappropriate to attempt to review all this information here. Interested readers are referred to the excellent review presented by Professor J.C. Jaeger in the eleventh Rankine lecture (1971).

In the context of this discussion, one of the most significant steps was a suggestion by Murrell (1958) that the brittle fracture criterion proposed by Griffith (1921,1924) could be applied to rock. Griffith postulated that, in brittle materials such as glass, fracture initiated when the tensile strength of the material is exceeded by stresses generated at the ends of microscopic flaws in the material. In rock, such flaws could be pre-existing cracks, grain boundaries or other discontinuities. Griffith's theory, summarized for rock mechanics application by Hoek (1968), predicts a parabolic Mohr failure envelope defined by the equation:

$$\tau = 2(|\sigma_t| (|\sigma_t| + \sigma'))^{1/2} \quad (1)$$

Where τ is the shear stress

σ' is the effective normal stress and

σ_t is the tensile strength of the material (note that tensile stresses are considered negative throughout this paper).

Griffith's theory was originally derived for predominantly tensile stress fields. In applying this criterion to rock subjected to compressive stress conditions, it soon became obvious that the frictional strength of closed crack has to be allowed for, and McClintock and Walsh (1962) proposed a modification to Griffith's theory to account for these frictional forces. The Mohr failure envelope for the modified Griffith theory is defined by the equation:

$$\tau = 2|\sigma_t| + \sigma' \tan \phi' \quad (2)$$

Where ϕ' is the angle of friction on the crack surfaces. (Note, this equation is only valid for $\sigma > 0$).

Strength of jointed rock masses

	Description	Strength characteristics	Strength testing	Theoretical considerations
	Hard intact rock	Brittle, elastic and generally isotropic	Triaxial testing of core specimens in laboratory relatively simple and inexpensive and results usually reliable	Theoretical behaviour of isotropic elastic brittle rock adequately understood for most practical applications
	Intact rock with single inclined discontinuity	Highly anisotropic, depending on shear strength and inclination of discontinuity	Triaxial testing of core with inclined joints difficult and expensive but results reliable. Direct shear testing of joints simple and inexpensive but results require careful interpretation	Theoretical behaviour of individual joints and of schistose rock adequately understood for most practical applications
	Massive rock with a few sets of discontinuities	Anisotropic, depending on number, shear strength and continuity of discontinuities	Laboratory testing very difficult because of sample disturbance and equipment size limitations	Behaviour of jointed rock poorly understood because of complex interaction of interlocking blocks
	Heavily jointed rock	Reasonably isotropic. Highly dilatant at low normal stress levels with particle breakage at high normal stress	Triaxial testing of undisturbed core samples extremely difficult due to sample disturbance and preparation problems	Behaviour of heavily jointed rock very poorly understood because of interaction of interlocking angular pieces
	Compacted rockfill	Reasonably isotropic. Less dilatant and lower shear strength than in situ jointed rock but overall behaviour generally similar	Triaxial testing simple but expensive because of large equipment size required to accommodate representative samples	Behaviour of compacted rockfill reasonably well understood from soil mechanics studies on granular materials
	Loose waste rock	Poor compaction and grading allow particle rotation and movement resulting in mobility of waste rock dumps	Triaxial or direct shear testing relatively simple but expensive because of large equipment size required	Behaviour of waste rock adequately understood for most applications

Figure 1 : Summary of range of rock mass characteristics

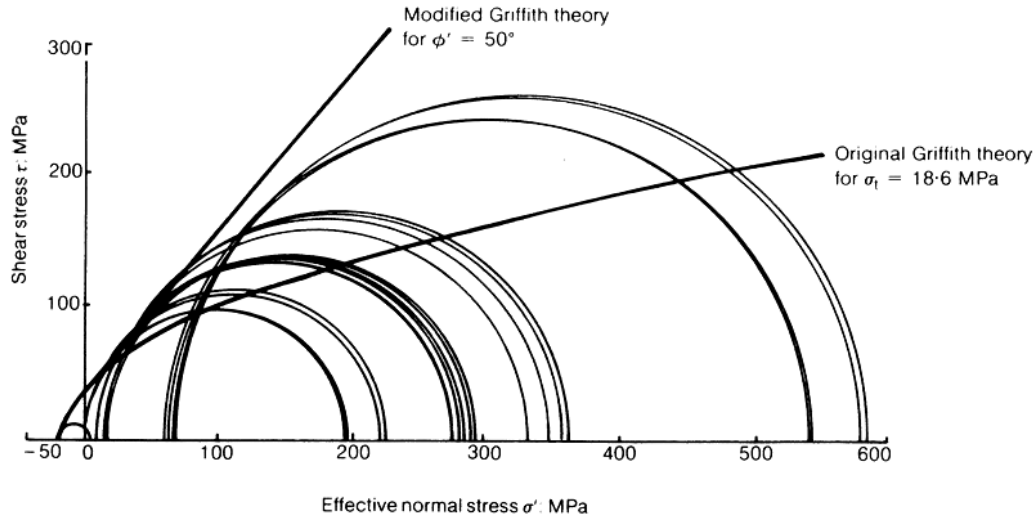


Figure 2 : Mohr circles for failure of specimens of quartzite tested by Hoek (1965). Envelopes included in the figure are calculated by means of the original and modified Griffith theories of brittle fracture initiation.

Detailed studies of crack initiation and propagation by Hoek and Bieniawski (1965) and Hoek (1968) showed that the original and modified Griffith theories are adequate for the prediction of fracture initiation in rocks but that they fail to describe fracture propagation and failure of a sample. Figure 2 gives a set of Mohr circles representing failure of the quartzite tested triaxially (Hoek, 1965). Included in this figure are Mohr envelopes calculated by means of equations 1 and 2 (for $\sigma_t = 18.6$ MPa and $\phi = 50^\circ$). It will be noted that neither of these curves can be considered acceptable envelopes to the Mohr circles representing failure of the quartzite under compressive stress conditions. In spite of the inadequacy of the specimens, a study of the mechanics of fracture initiation and of the shape of the Mohr envelopes predicted by these theories was a useful starting point in deriving the empirical failure criterion discussed in this chapter.

Jaeger (1971), in discussing failure criteria for rock, comments that 'Griffith theory has proved extraordinarily useful as a mathematical model for studying the effect of cracks on rock, but it is essentially only a mathematical model; on the microscopic scale rocks consist of an aggregate of anisotropic crystals of different mechanical properties and it is these and their grain boundaries which determine the microscopic behaviour'

Recognition of the difficulty involved in developing a mathematical model which adequately predicts fracture propagation and failure in rock led a number of authors to propose empirical relationships between principal stresses or between shear and normal stresses at failure. Murrell (1965), Hoek (1968), Hobbs (1970) and Bieniawski (1974) all proposed different forms of empirical criteria. The failure criterion put forward here is based on that presented by Hoek and Brown (1980a, 1980b) and resulted from their efforts to produce an acceptable failure criterion for the design of underground excavations in rock.

An empirical failure criterion for rock

In developing their empirical failure criterion, Hoek and Brown (1980a) attempted to satisfy the following conditions:

- (a) The failure criterion should give good agreement with experimentally determined rock strength values.
- (b) The failure criterion should be expressed by mathematically simple equations based, to the maximum extent possible, upon dimensionless parameters.
- (c) The failure criterion should offer the possibility of extension to deal with anisotropic failure and the failure of jointed rock masses.

The studies on fracture initiation and propagation, discussed earlier, suggested that the parabolic Mohr envelope predicted by the original Griffith theory adequately describes both fracture initiation and failure of brittle materials under conditions where the effective normal stress acting across a pre-existing crack is tensile (negative). This is because fracture propagation follows very quickly upon fracture initiation under tensile stress conditions, and hence fracture initiation and failure of the specimen are practically indistinguishable.

Figure 2 shows that, when the effective normal stress is compressive (positive), the envelope to the Mohr circles tends to be curvilinear, but not to the extent predicted by the original Griffith theory.

Based on these observations, Hoek and Brown (1980a) experimented with a number of distorted parabolic curves to find one which gave good coincidence with the original Griffith theory for tensile effective normal stresses, and which fitted the observed failure conditions for brittle rocks subjected to compressive stress conditions.

Note that the process used by Hoek and Brown in deriving their empirical failure criterion was one of pure trial and error. Apart from the conceptual starting point provided by Griffith theory, there is no fundamental relationship between the empirical constants included in the criterion and any physical characteristics of the rock. The justification for choosing this particular criterion over the numerous alternatives lies in the adequacy of its predictions of observed rock fracture behaviour, and the convenience of its application to a range of typical engineering problems.

As stated earlier, the author's background in designing underground excavations in rock resulted in the decision to present the failure criterion in terms of the major and minor principal stresses at failure. The empirical equation defining the relationship between these stresses is

$$\sigma_1' = \sigma_3' + (m\sigma_c\sigma_3' + s\sigma_c^2)^{1/2} \quad (3)$$

where σ_1' is the major principal effective stress at failure

σ_3' is the minor principal effective stress or, in the case of a triaxial test, the confining pressure

σ_c is the uniaxial compressive strength of the intact rock material from which the rock mass is made up

Strength of jointed rock masses

m and s are empirical constants

The constant m always has a finite positive value which ranges from about 0.001 for highly disturbed rock masses, to about 25 for hard intact rock. The value of the constant s ranges from 0 for jointed masses, to 1 for intact rock material.

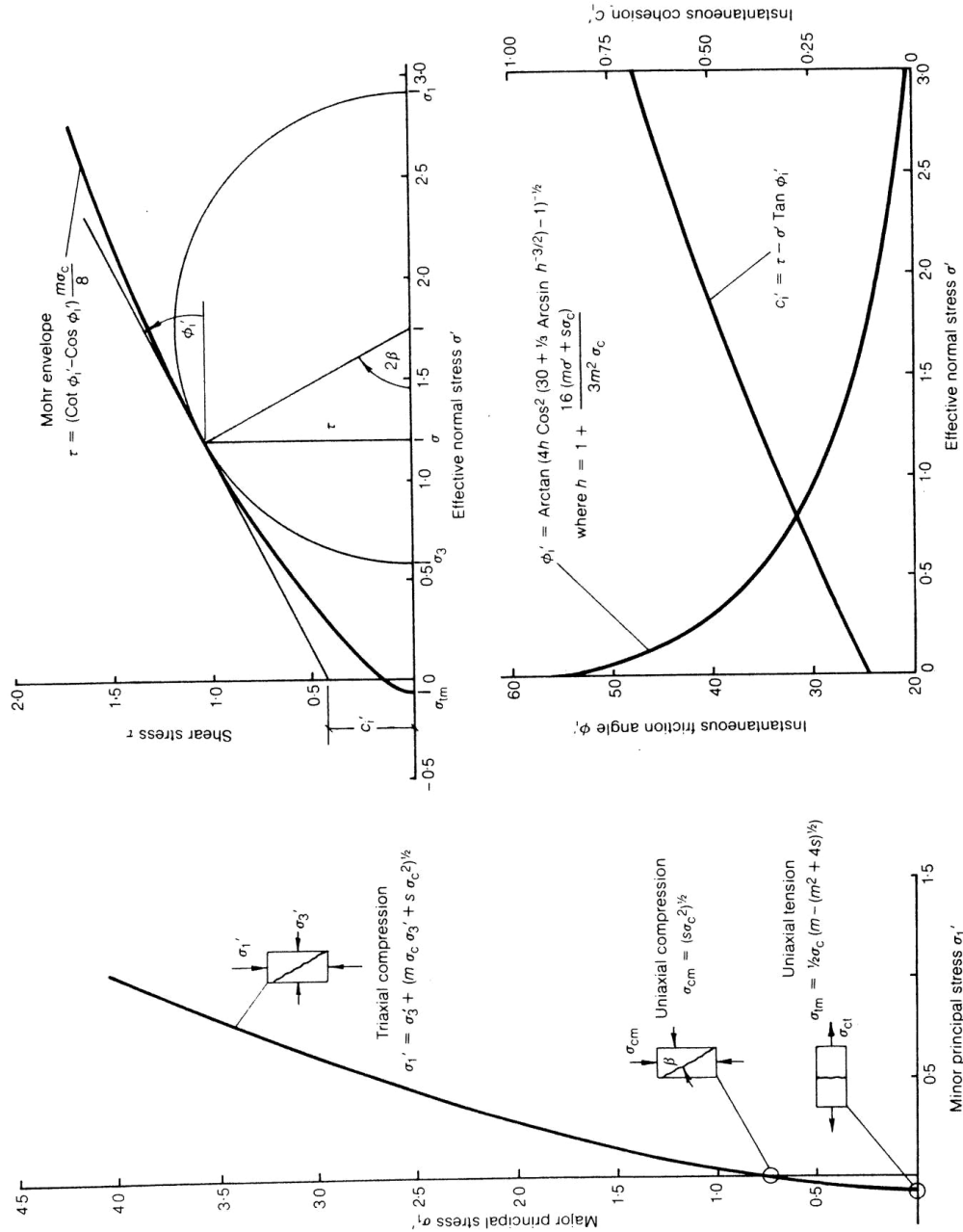


Figure 3. Summary of equations with the non-linear failure criterion proposed by Hoek & Brown (1980b)

Strength of jointed rock masses

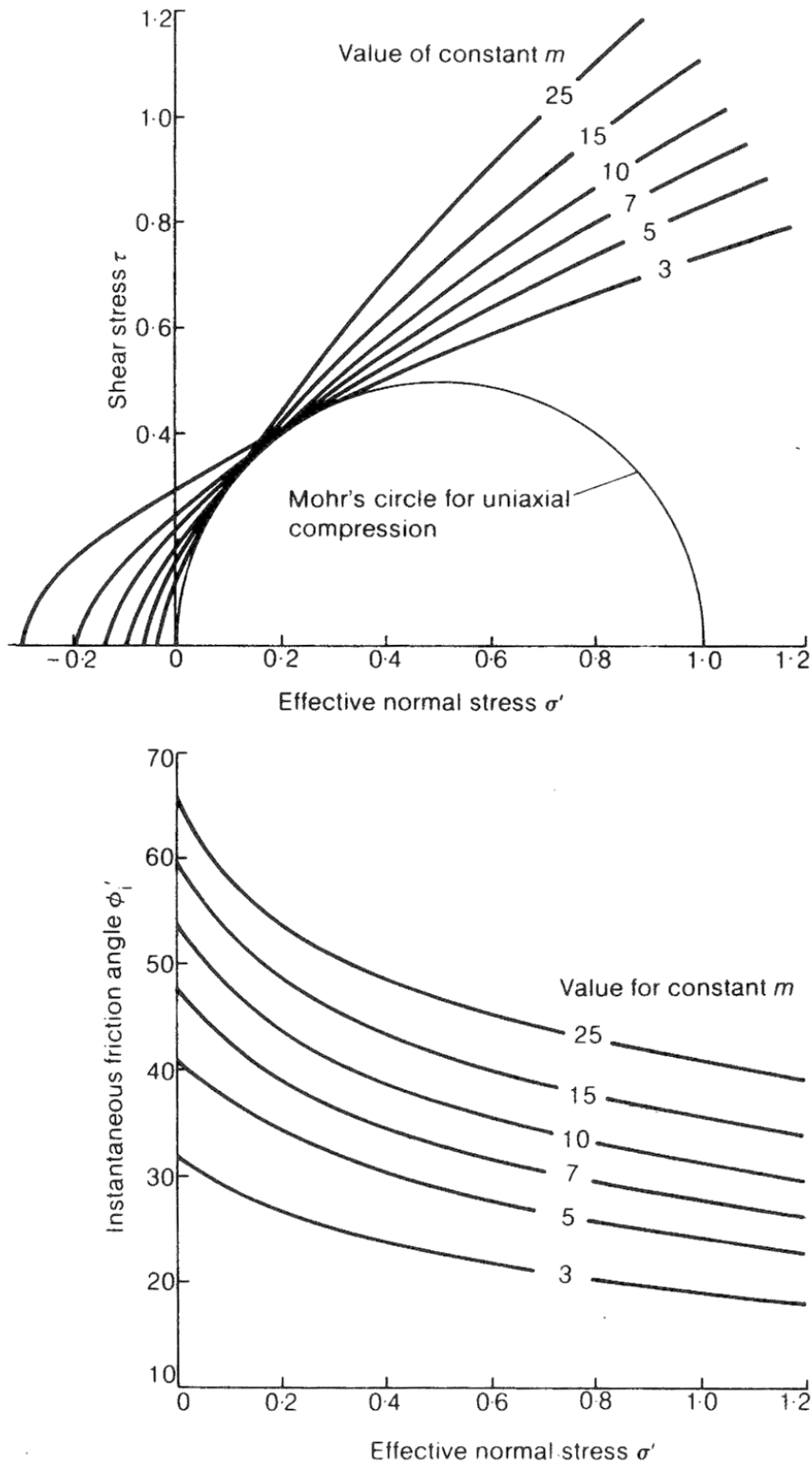


Figure 4. Influence of the value of the constant m on the shape of the Mohr failure envelope and on the instantaneous friction angle at different effective normal stress levels.

Substitution of $\sigma_3' = 0$ into equation 3 gives the unconfined compressive strength of a rock mass as

$$\sigma_1' = \sigma_c = (s\sigma_c^2)^{1/2} \quad (4)$$

Similarly, substitution $\sigma_1' = 0$ in equation 3, and solution of the resulting quadratic equation for σ_3' , gives the uniaxial tensile strength of a rock mass as

$$\sigma_3' = \sigma_t = \frac{1}{2}\sigma_c \left(m - (m^2 + 4s)^{1/2} \right) \quad (5)$$

The physical significance of equations 3, 4 and 5 is illustrated in the plot of σ_1' versus σ_3' given in figure 3.

While equation 3 is very useful in designing underground excavations, where the response of individual rock elements to in situ and induced stresses is important, it is of limited value in designing rock slopes where the shear strength of a failure surface under specified effective normal stress conditions is required.

The Mohr failure envelope corresponding to the empirical failure criterion defined by equation 3 was derived by Dr. John Bray of Imperial College and is given by:

$$\tau = (\text{Cot } \phi_i' - \text{Cos } \phi_i') \frac{m\sigma_c}{8} \quad (6)$$

where τ is the shear stress at failure

ϕ_i' is the instantaneous friction angle at the given values of τ and σ'
i.e. the inclination of the tangent to the Mohr failure envelope at the point (σ', τ) as shown in figure 3.

The value of the instantaneous friction angle ϕ_i' is given by:

$$\phi_i' = \text{Arc tan} \left(4h \text{Cos}^2 \left(30 + \frac{1}{3} \text{Arc sin } h^{-3/2} \right) - 1 \right)^{-1/2} \quad (7)$$

where

$$h = 1 + \frac{16(m\sigma' + s\sigma_c)}{3m^2\sigma_c}$$

and σ' is the effective normal stress.

The instantaneous cohesive strength c_i' , shown in figure 3, is given by:

$$c_i' = \tau - \sigma' \text{Tan } \phi_i' \quad (8)$$

From the Mohr circle construction given in figure 3, the failure plane inclination β is given by

$$\beta = 45 - \frac{1}{2}\phi_i' \quad (9)$$

An alternative expression for the failure plane inclination, in terms of the principal stresses σ_1' and σ_3' , was derived by Hoek and Brown (1980a):

$$\beta = \frac{1}{2} \text{Arc sin} \frac{\tau_m}{\tau_m + m\sigma_c/8} (1 + m\sigma_c/4\tau_m)^{1/2} \quad (10)$$

where $\tau = 1/2(\sigma_1' - \sigma_3')$.

Characteristics of empirical criterion

The empirical failure criterion presented in the preceding section contains three constants m , s and σ_c . The significance of each of these will be discussed in turn later.

Constants m and s are both dimensionless and are very approximately analogous to the angle of friction, ϕ , and the cohesive strength, c' , of the conventional Mohr-Coulomb failure criterion.

Figure 4 illustrates the influence of different values of the constant m upon the Mohr failure envelope for intact rock. Note that in plotting these curves, the values of both s and σ_c are assumed equal to unity.

Large values of m , in the order of 15 to 25, give steeply inclined Mohr envelopes and high instantaneous friction angles at low effective normal stress levels. These large m values tend to be associated with brittle igneous and metamorphic rocks such as andesites, gneisses and granites. Lower m values, in the order of 3 to 7, give lower instantaneous friction angles and tend to be associated with more ductile carbonate rocks such as limestone and dolomite.

The influence of the value of the constant s upon the shape of the Mohr failure envelope and upon the instantaneous friction angle at different effective normal stress levels is illustrated in figure 5. The maximum value of s is 1.00, and this applies to intact rock specimens which have a finite tensile strength (defined by equation 5). The minimum value of s is zero, and this applies to heavily jointed or broken rock in which the tensile strength has been reduced to zero and where the rock mass has zero cohesive strength when the effective normal stress is zero.

The third constant, σ_c , the uniaxial compressive strength of the intact rock material, has the dimensions of stress. This constant was chosen after very careful consideration of available rock strength data. The unconfined compressive strength is probably the most widely quoted constant in rock mechanics, and it is likely that an estimate of this strength will be available in cases where no other rock strength data are available.

Strength of jointed rock masses

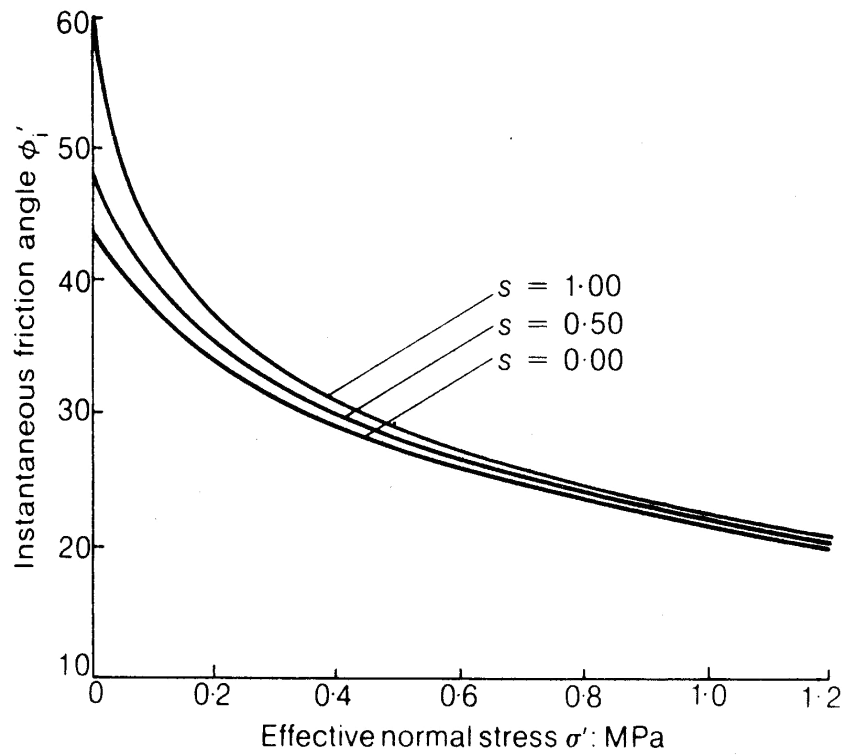
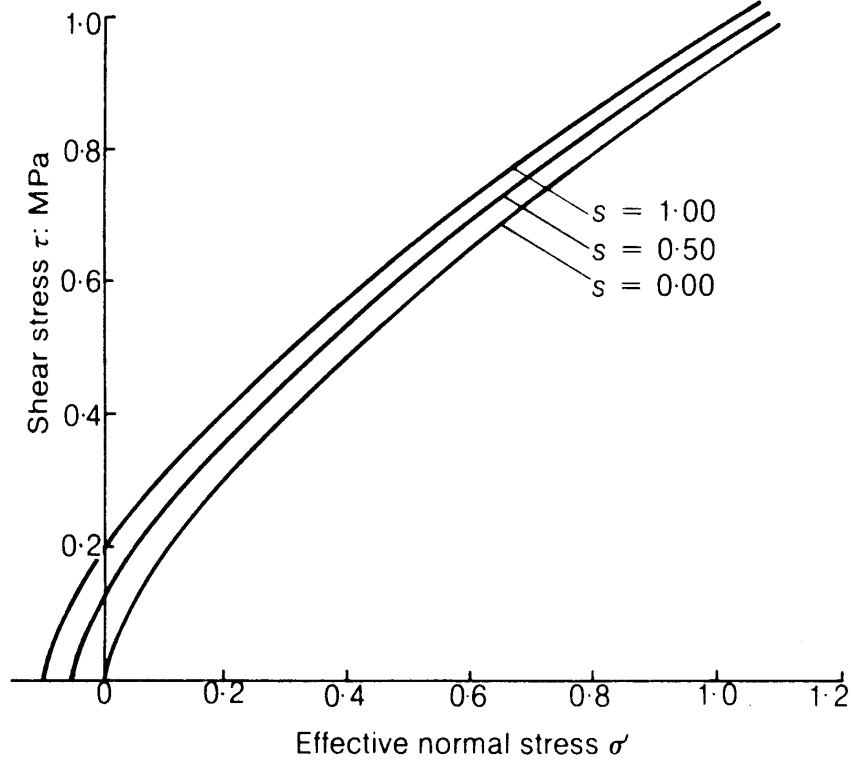


Figure 5. Influence of the value of the constant s on the shape of the Mohr failure envelope and on the instantaneous friction angle at different effective stress levels

Consequently, it was decided that the uniaxial compressive strength σ_c would be adopted as the basic unit of measurement in the empirical failure criterion.

Note that the failure criterion defined by equation 3 can be made entirely dimensionless by dividing both sides by the uniaxial compressive strength:

$$\sigma_1' / \sigma_c = \sigma_3' / \sigma_c + (m\sigma_3' / \sigma_c + s)^{1/2} \quad (11)$$

This formulation, which can also be achieved by simply putting $\sigma_c = 1$ in equation 3, is very useful when comparing the shape of Mohr failure envelopes for different rock materials.

A procedure for the statistical determination of the values of the constants m , s and σ_c from experimental data is given in appendix 1.

Triaxial data for intact rock

Hoek and Brown (1980a) analyzed published data from several hundred triaxial tests on intact rock specimens and found some useful trends. These trends will be discussed in relationship to two sets of data plotted as Mohr failure circles in figure 6. The sources of the triaxial data plotted in figure 6 are given in table 1.

Figure 6a gives Mohr failure envelopes for five different granites from the USA and UK. Tests on these granites were carried out in five different laboratories using entirely different triaxial equipment. In spite of these differences, the failure characteristics of these granites follow a remarkably consistent pattern, and the Mohr failure envelope predicted by equations 6 and 7 (for $\sigma_c = 1$, $m = 29.2$, and $s = 1$) fits all of these Mohr circles very well. Table 1 shows that a correlation coefficient of 0.99 was obtained by statistically fitting the empirical failure criterion defined by equation 3 to all of the granite strength data. The term granite defines a group of igneous rocks having very similar mineral composition, grain size and angularity, hence it is not too surprising that the failure characteristics exhibited by these rocks should be very similar, irrespective of the source of the granite. The trend illustrated in figure 6a has very important practical implications, since it suggests that it should be possible, given a description of the rock and an estimate of its uniaxial compressive strength, to predict its Mohr failure envelope with a relatively high degree of confidence. This is particularly important in early conceptual or feasibility studies where the amount of reliable laboratory data is very limited.

In contrast to the trends illustrated in figure 6a for granite, the plot given in figure 6b for limestone is less convincing. In this case, eleven different limestones, tested in three different laboratories, have been included in the plot. Table 1 shows that the values of the constant m , derived from statistical analyses of the test data, vary from 3.2 to 14.1, and that the correlation coefficient for the complete data set is only 0.68.

The scatter of the data included in figure 6b is attributed to the fact that the generic term limestone applies to a range of carbonate rocks formed by deposition of a variety of organic and inorganic materials. Consequently, mineral composition, grain size and

shape, and the nature of cementing materials between the grains will vary from one limestone to another.

Comparison of the two plots given in figure 6 suggests that the empirical failure criterion presented in this paper gives a very useful indication of the general trend of the Mohr failure envelope for different rock types. The accuracy of each prediction will depend upon the adequacy of the description of the particular rock under consideration. In comparing the granites and limestones included in figure 6, there would obviously be a higher priority in carrying out confirmatory laboratory tests on the limestone than on the granite.

Hoek and Brown (1980) found that there were definite trends which emerged from the statistical fitting of their empirical failure criterion (equation 3) to published triaxial data. For intact rock (for which $s = 1$), these trends are characterized by the value of the constant s which, as illustrated in figure 4, defines the shape of the Mohr failure envelope. The trends suggested by Hoek and Brown (1980) are as follows:

- a) Carbonate rocks with well-developed crystal cleavage (dolomite, limestone and marble): $m = 7$
- b) Lithified argillaceous rocks (mudstone, shale and slate (normal to cleavage)): $m = 10$
- c) Arenaceous rocks with strong crystals and poorly developed crystal cleavage (sandstone and quartzite): $m = 15$
- d) Fine grained polyminerallic igneous crystalline rocks (andesite, dolerite, diabase and rhyotite): $m = 17$
- e) Coarse grained polyminerallic igneous and metamorphic rocks (amphibolite, gabbro, gneiss, granite, norite and granodiorite): $m = 25$

Before leaving the topic of intact rock strength, the fitting of the empirical failure criterion defined by equation 3 to a particular set of triaxial data is illustrated in figure 7. The Mohr circles plotted in this figure were obtained by Bishop and Garga (1969) from a series of carefully performed triaxial tests on undisturbed samples of London clay (Bishop et al, 1965). The Mohr envelope plotted in figure 7 was determined from a statistical analysis of Bishop and Garga's data (using the technique described in appendix 1), and the values of the constants are $\sigma_c = 211.8$ kPa, $m = 6.475$ and $\sigma_c = 1$. The correlation coefficient for the fit of the empirical criterion to the experimental data is 0.98.

This example was chosen for its curiosity value rather than its practical significance, and because of the strong association between the British Geotechnical Society and previous Rankine lecturers and London clay. The example does serve to illustrate the importance of limiting the use of the empirical failure criterion to a low effective normal stress range. Tests on London clay at higher effective normal stress levels by Bishop et al (1965) gave approximately linear Mohr failure envelopes with friction angles of about 11° .

As a rough rule-of-thumb, when analyzing intact rock behaviour, the author limits the use of the empirical failure criterion to a maximum effective normal stress level equal to the unconfined compressive strength of the material. This question is examined later in a discussion on brittle-ductile transition in intact rock.

Table 1. Sources of data included in Figure 6*

Rock type	Location	Reference	Number tested	Uniaxial compressive strength		Each sample		Rock type	
				lb/in ²	MPa	m	r ² †	m	r ² †
Granite	Westerley, USA	Heard <i>et al.</i> (1974)	17	31 040	2140	26.7	1.00		
	Westerley, USA	Wawersik & Brace (1971)	7	43 310	298.6	27.0	1.00		
	Westerley, USA	Brace (1964)	7	49 820	343.5	28.3	0.98		
	Westerley, USA	Mogi (1967)	6	32 440	223.7	32.8	0.99		
	Stone Mountain, USA	Schwartz (1964)	14	16 850	116.2	28.9	0.93	29.2	0.99
	Blackingstone, UK	Franklin & Hoek (1970)	48	30 410	209.7	20.8	0.91		
	Mount Sorrel, UK	Misra (1972)	5	39 910	275.2	26.5	0.99		
	Carnarvon, Redruth, UK	Misra (1972)	5	23 540	162.3	27.7	0.99		
	Portland, UK	Franklin & Hoek (1970)	30	13 300	91.7	7.5	0.72		
	Indiana, USA	Schwartz (1964)	6	7090	48.9	3.2	0.95		
	Bath, UK	Misra (1972)	7	6830	47.1	5.5	0.97		
	Grindling Stubbs, UK	Misra (1972)	6	19 450	134.1	8.8	0.97		
	Kirbymoorside, UK	Misra (1972)	5	23 830	164.3	12.3	0.98		
	Blackwell, UK	Misra (1972)	5	29 211	201.4	10.0	0.92	5.4	0.68
Foster Yeoman, UK	Misra (1972)	5	24 265	167.3	14.1	0.95			
Giggleswick, UK	Misra (1972)	5	22 423	154.6	8.8	0.97			
Kelmac, UK	Misra (1972)	5	16 897	116.5	7.3	1.00			
Threshfield, UK	Misra (1972)	5	21 423	147.7	6.9	0.98			
Swinden Cracoe, UK	Misra (1972)	5	16 027	110.5	8.4	0.96			

* Material constant $s = 1$ for intact rock.

† r^2 is coefficient of determination or correlation coefficient.

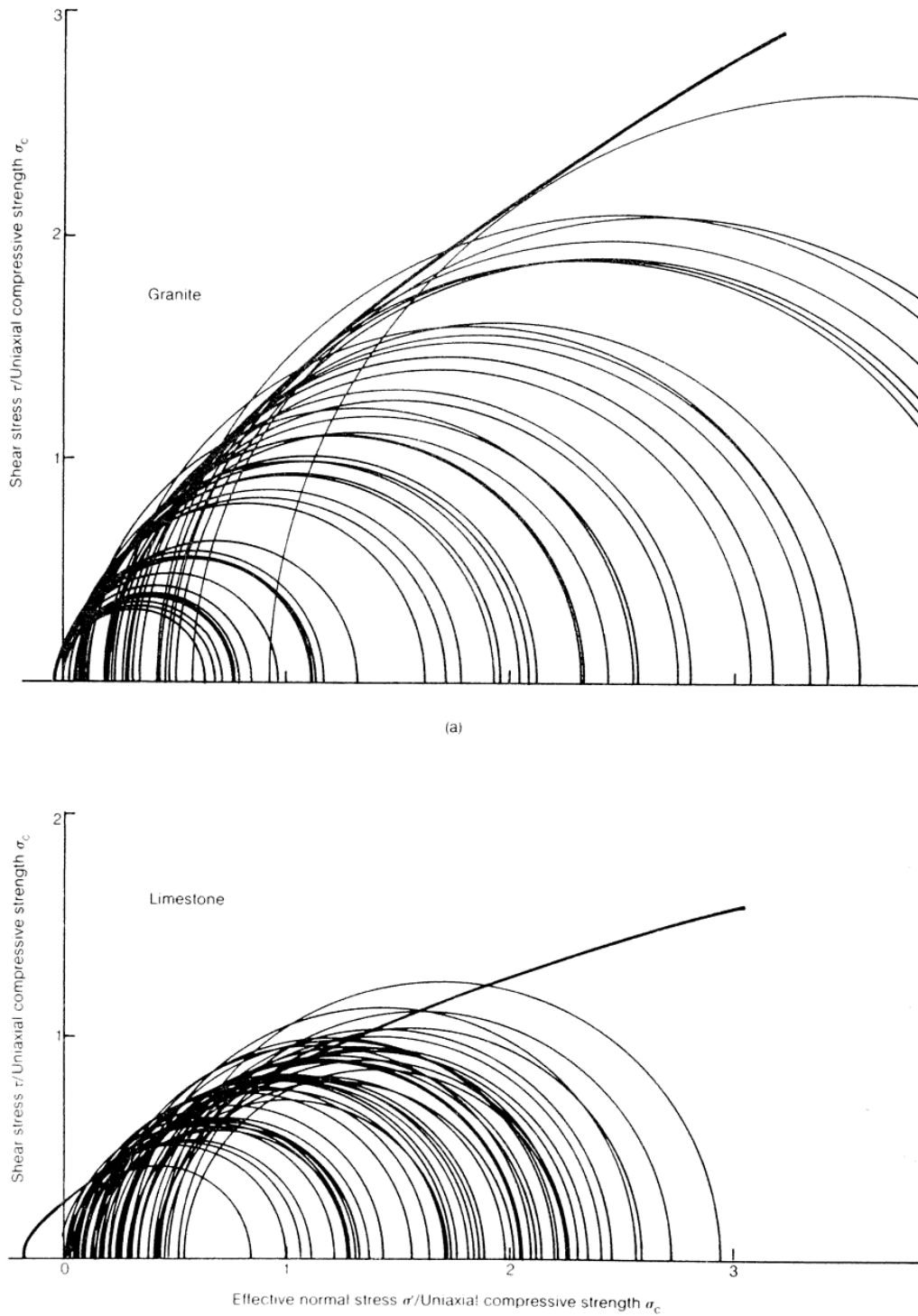


Figure 6 : Mohr failure circles for published triaxial test data for intact samples of (a) granite and (b) limestone.

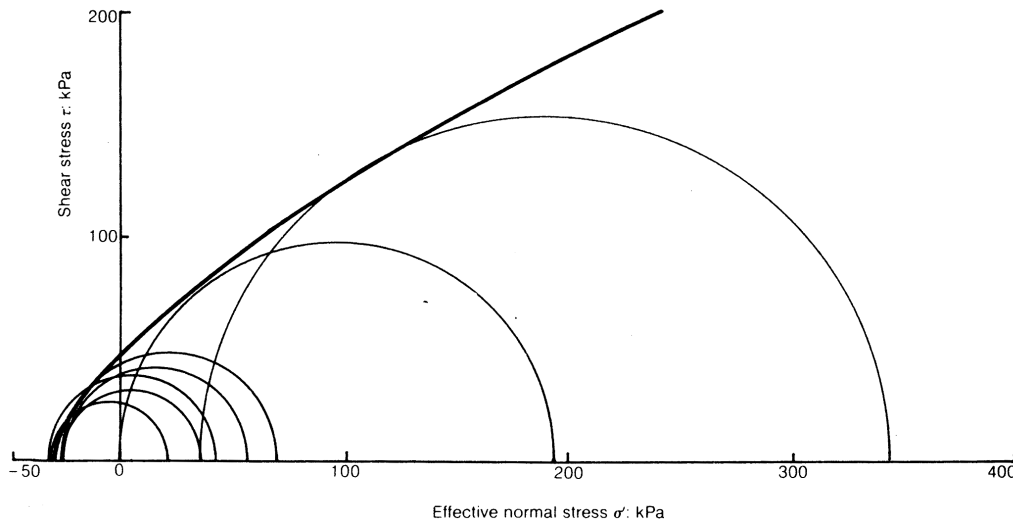


Figure 7 : Mohr failure envelope for drained triaxial tests at very low normal stress levels carried out by Bishop and Garga (1969) on undisturbed samples of London clay.

Assumptions included in empirical failure criterion

A number of simplifying assumptions have been made in deriving the empirical failure criterion, and it is necessary briefly to discuss these assumptions before extending the criterion to deal with jointed rock masses.

Effective stress

Throughout this discussion, it is assumed that the empirical failure criterion is valid for effective stress conditions. In other words, the effective stress σ' used in equations 7 and 8 is obtained from $\sigma' = \sigma - u$, where σ is the applied normal stress and u is the pore or joint water pressure in the rock. In spite of some controversy on this subject, discussed by Jaeger and Cook (1969), Brace and Martin (1969) demonstrate that the effective stress concept appears to be valid in intact rocks of extremely low permeability, provided that loading rates are sufficiently low to permit pore pressures to equalize. For porous rocks such as sandstone, normal laboratory loading rates will generally satisfy effective stress conditions (Handin et al, (1963)) and there is no reason to suppose that they will not apply in the case of jointed rocks.

Influence of pore fluid on strength

In addition to the influence of pore pressure on strength, it is generally accepted that the pore fluid itself can have a significant influence on rock strength. For example, Colback and Wiid (1965) and Broch (1974) showed that the unconfined compressive strength of quartzitic shale, quartzdiorite, gabbro and gneiss can be reduced by as much as 2 by saturation in water as compared with oven dried specimens. Analyses of their results suggest that this reduction takes place in the unconfined compressive strength σ_c and not in the constant m of the empirical failure criterion.

It is important, in testing rock materials or in comparing data from rock strength tests,

that the moisture content of all specimens be kept within a narrow range. In the author's own experience in testing samples of shale which had been left standing on the laboratory shelf for varying periods of time, the very large amount of scatter in strength data was almost eliminated by storing the specimens in a concrete curing room to bring them close to saturation before testing. Obviously, in testing rocks for a particular practical application, the specimens should be tested as close to in situ moisture content as possible.

Influence of loading rate

With the exception of effective stress tests on very low porosity materials (e.g. Brace and Martin (1968)), or tests on viscoelastic materials such as salt or potash, it is generally assumed that the influence of loading rate is insignificant when dealing with rock. While this may be an oversimplification, the author believes that it is sufficiently accurate for most practical applications.

Influence of specimen size

Hoek and Brown (1980a) have analyzed the influence of specimen size on the results of strength tests on the intact rock samples. They found that the influence of specimen size can be approximated by the relationship

$$\sigma_c = \sigma_{c50} (50/d)^{0.18} \quad (12)$$

where σ_c is the unconfined compressive strength,
 d is the diameter of the specimen in millimeters, and
 σ_{c50} is the unconfined compressive strength of a 50 mm diameter specimen of the same material.

In the case of jointed rocks, the influence of size is controlled by the relationship between the spacing of joints and the size of the sample. This problem is dealt with in the discussion on jointed rock masses given later in this paper.

Influence of intermediate principal stress

In deriving the empirical failure criterion presented in this paper, Hoek and Brown (1980) assumed that the failure process is controlled by the major and minor principal stresses σ'_1 and σ'_3 , and that the intermediate principal stress σ'_2 has no significant influence upon this process. This is almost certainly an over-simplification, but there appears to be sufficient evidence (reviewed by Jaeger and Cook (1967)) to suggest that the influence of the intermediate principle stress can be ignored without introducing unacceptably large errors.

Failure surface inclination

The inclination of an induced failure plane in an intact rock specimen is given by equation 9 or equation 10. Note that this inclination is measured from the direction of the maximum principal stress σ'_1 , as illustrated in figure 3.

The results of a series of triaxial tests by Wawersik (1968) on Tennessee marble are listed in table 2, and plotted as Mohr circles in figure 8. Also listed in table 2 and plotted in figure 8, are observed failure plane inclinations.

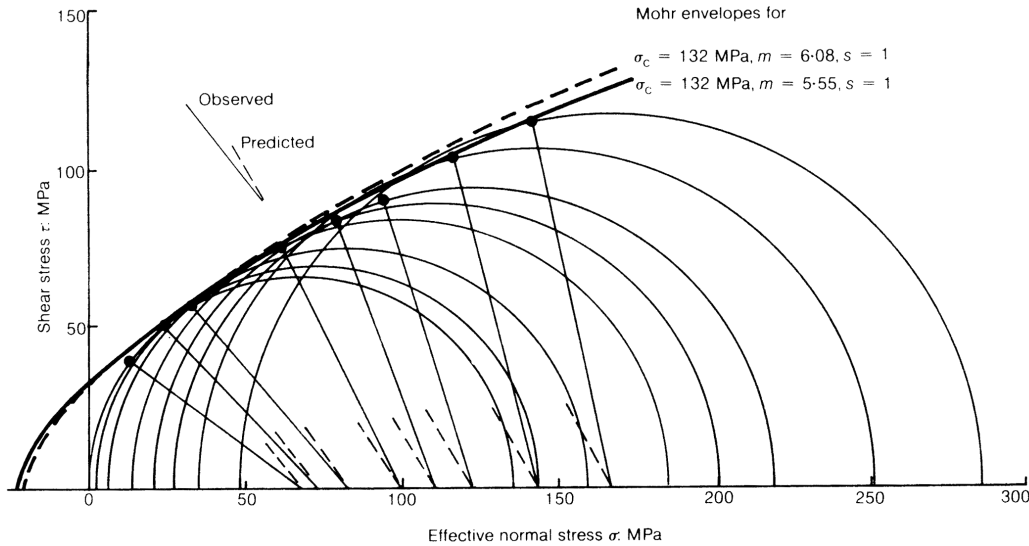


Figure 8 : Plot of Mohr failure circles for Tennessee marble tested by Wawersik (1968) giving comparison between predicted and observed failure plane inclination.

Table 2. Observed and predicted failure plane inclination for Tennessee marble (Wawersik, 1968).

Confining pressure: MPa	Axial strength: MPa	Observed fracture angle	Predicted fracture angle
0	134.48	18.0	26.61
3.45	143.45	23.4	27.0
6.90	160.00	24.8	27.7
13.79	186.21	31.7	28.7
20.69	201.38	35.1	29.1
27.59	220.00	36.3	29.7
34.48	251.03	37.8	30.6
48.28	286.21	38.8	31.4

A statistical analysis of the triaxial test data gives the following constants: $\sigma_c = 132.0$ MPa, $m = 6.08$, $s = 1$, with a correlation coefficient of 0.99. The Mohr envelope defined by these constants is plotted as a dashed curve in figure 8.

The predicted fracture angles listed in Table 2 have been calculated for $\sigma_c = 132.0$ MPa and $m = 6.08$ by means of equation 10, and it will be noted that there are significant differences between observed and predicted fracture angles.

On the other hand, a Mohr envelope fitted through the shear stress (τ) and effective normal stress (σ') points defined by construction (using the Mohr circles), gives a value of $m = 5.55$ for $\sigma_c = 132$ MPa and $s = 1.00$. The resulting Mohr envelope, plotted as a full line in figure 8, is not significantly different from the Mohr envelope determined by analysis of the principal stresses.

These findings are consistent with the author's own experience in rock testing. The fracture angle is usually very difficult to define, and is sometimes obscured altogether. This is because, as discussed earlier in this paper, the fracture process is complicated and does not always follow a clearly defined path. When the failure plane is visible, the inclination of this plane cannot be determined to better than plus or minus 5° . In contrast, the failure stresses determined from a carefully conducted set of triaxial tests are usually very clearly grouped, and the pattern of Mohr circles plotted in figure 8 is not unusual in intact rock testing.

The conclusion to be drawn from this discussion is that the failure plane inclinations predicted by equations 9 or 10 should be regarded as approximate only, and that, in many rocks, no clearly defined failure surfaces will be visible.

Brittle-ductile transition

The results of a series of triaxial tests carried out by Schwartz (1964) on intact specimens of Indiana limestone are plotted in figure 9. A transition from brittle to ductile behaviour appears to occur at a principal stress ratio of approximately $\sigma'_1 / \sigma'_3 = 4.3$.

A study of the failure characteristics of a number of rocks by Mogi (1966) led him to conclude that the brittle-ductile transition for most rocks occurs at an average principal stress ratio $\sigma'_1 / \sigma'_3 = 3.4$.

Examination of the results plotted in figure 9, and of similar results plotted by Mogi, shows that there is room for a wide variety of interpretations of the critical principal stress ratio, depending upon the curve fitting procedure employed and the choice of the actual brittle-ductile transition point. The range of possible values of σ'_1 / σ'_3 appears to lie between 3 and 5.

A rough rule-of-thumb used by this author is that the confining pressure σ'_1 must always be less than the unconfined compressive strength σ_c of the material for the behaviour to be considered brittle. In the case of materials characterized by very low values of the constant m , such as the Indiana limestone considered in figure 9 ($m = 3.2$), the value of $\sigma'_1 = \sigma_c$ may fall beyond the brittle-ductile transition. However, for most rocks encountered in practical engineering applications, this rule-of-thumb appears to be adequate.

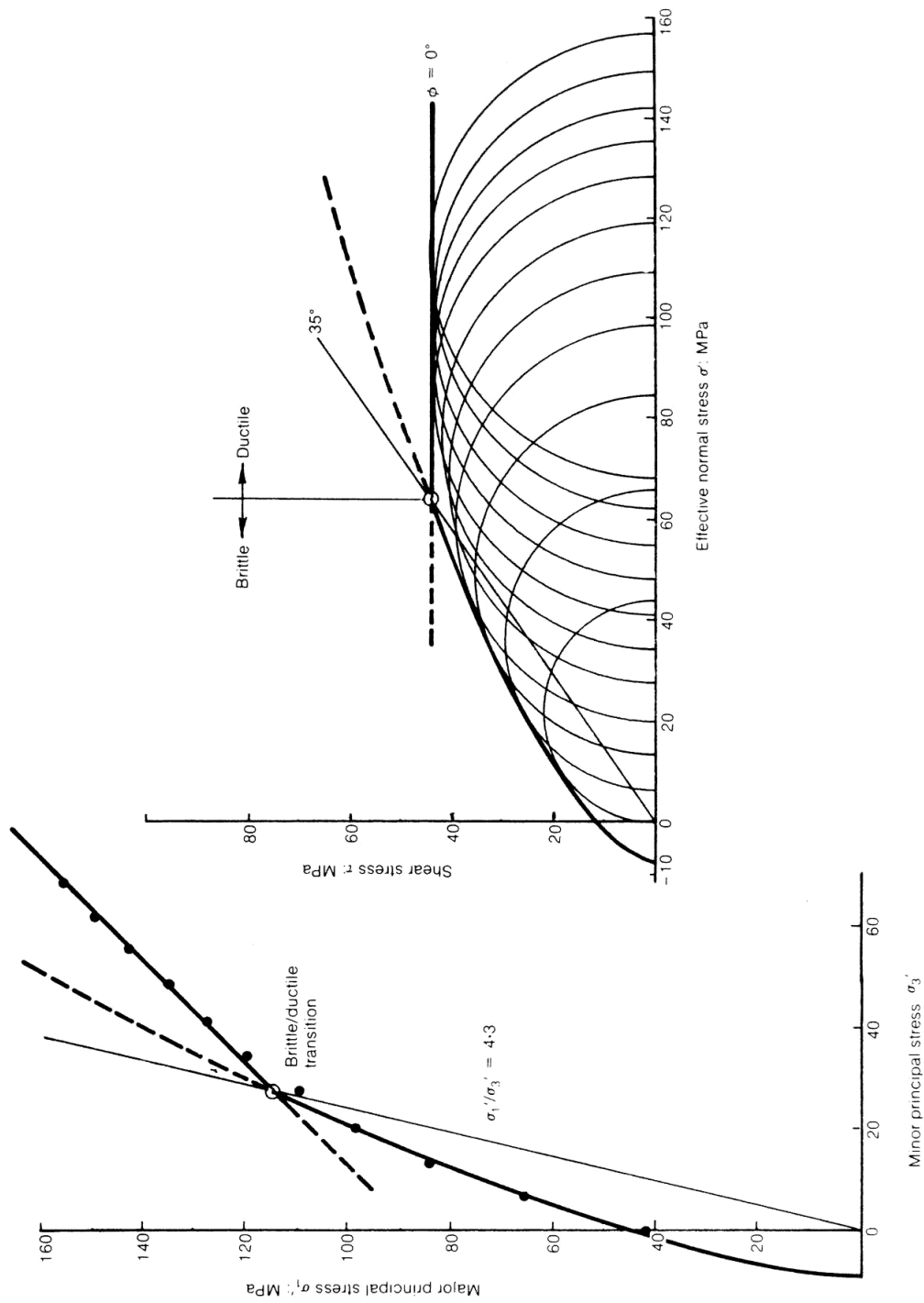


Figure 9. Results of triaxial tests on Indiana limestone carried out by Schwartz (1964) illustrating the brittle-ductile transition.

Shear strength of discontinuities

The shear strength of discontinuities in rock has been extensively discussed by a

number of authors such as Patton (1966), Goodman (1970), Ladanyi and Archambault (1970), Barton (1971, 1973, 1974), Barton and Choubey (1977), and Richards and Cowland (1982). These discussions have been summarized by Hoek and Bray (1981).

For practical field applications involving the estimation of the shear strength of rough discontinuity surfaces in rock, the author has no hesitation in recommending the following empirical relationship between shear strength (τ) and effective normal stress (σ') proposed by Barton (1971, 1973).

$$\tau = \sigma' \tan(\phi'_b + JRC \log_{10}(JCS / \sigma')) \quad (13)$$

where ϕ'_b is the 'basic' friction angle of smooth planar discontinuities in the rock under consideration, JRC is a joint roughness coefficient which ranges from 5 for smooth surfaces, to 20 for rough undulating surfaces, and JCS is joint wall compressive strength which, for clean unweathered discontinuities, equals the uniaxial compressive strength of the intact rock material.

While Barton's equation is very useful for field applications, it is by no means the only one which can be used for fitting to laboratory shear test data such as that published by Krsmanovic (1967), Martin and Miller (1974), and Hencher and Richards (1982).

Figure 10 gives a plot of direct shear strength data obtained by Martin and Miller (1974) from tests on 150 mm by 150 mm joint surfaces in moderately weathered greywacke (grade 3, test sample number 7). Barton's empirical criterion (equation 13) was fitted by trial and error, and the dashed curve plotted in figure 10 is defined by $\phi'_b = 20^\circ$, $JRC = 17$, and $JCS = 20$ MPa.

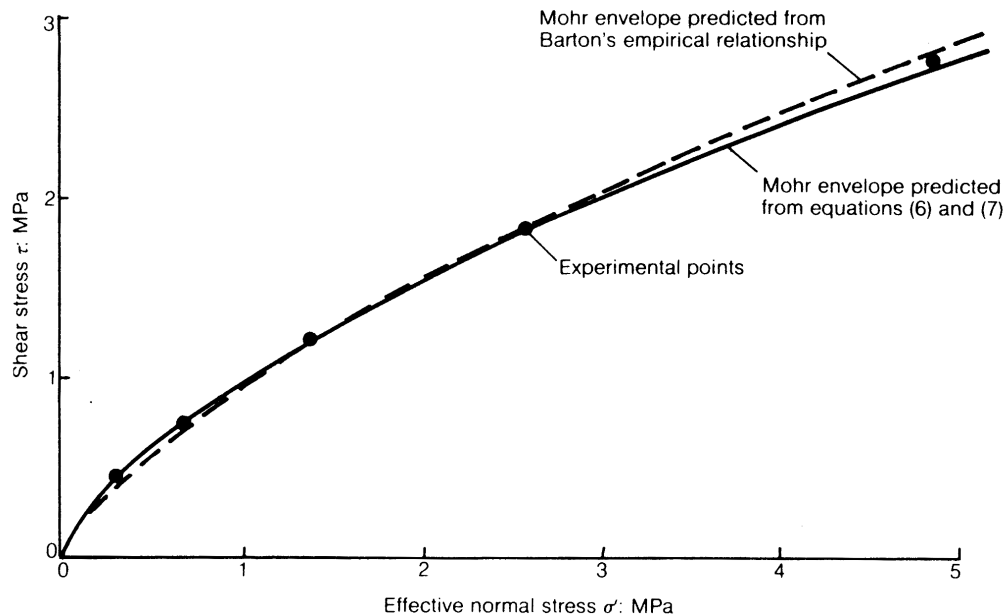


Figure 10 : Results of direct shear tests on moderately weathered greywacke, tested by Martin and Miller (1974), compared with empirical failure envelopes

Also included in figure 10 is a Mohr envelope defined by equations 6 and 7 in this paper for $\sigma_c = 20$ MPa, $m = 0.58$ and $s = 0$ (determined by the method described in appendix 1). It will be seen that this curve is just as good a fit to the experimental data as Barton's curve.

A number of analyses, such as that presented in Figure 10, have convinced the author that equations 6 and 7 provide a reasonably accurate prediction of the shear strength of rough discontinuities in rock under a wide range of effective normal stress conditions. This fact is useful in the study of schistose and jointed rock mass strength which follows.

Strength of schistose rock

In the earlier part of these notes, the discussion on the strength of intact rock was based upon the assumption that the rock was isotropic, i.e. its strength was the same in all directions. A common problem encountered in rock mechanics involves the determination of the strength of schistose or layered rocks such as slates or shales.

If it is assumed that the shear strength of the discontinuity surfaces in such rocks is defined by an instantaneous friction angle ϕ'_i and an instantaneous cohesion c'_i (see figure 3), then the axial strength σ'_1 of a triaxial specimen containing inclined discontinuities is given by the following equation (see Jaeger and Cook (1969), pages 65 to 68):

$$\sigma'_1 = \sigma'_3 + \frac{2(c'_i + \sigma'_3 \tan \phi'_i)}{(1 - \tan \phi'_i \tan \beta) \sin 2\beta} \quad (14)$$

where σ'_3 is the minimum principal stress or confining pressure, and β is the inclination of the discontinuity surfaces to the direction of the major principal stress σ_1 as shown in figure 11a.

Equation 14 can only be solved for values of β within about 25° of the friction angle ϕ'_i . Very small values of β will give very high values for σ'_1 , while values of β close to 90° will give negative (and hence meaningless) values for σ'_1 . The physical significance of these results is that slip on the discontinuity surfaces is not possible, and failure will occur through the intact material as predicted by equation 3. A typical plot of the axial strength σ'_1 versus the angle β is given in figure 11b.

If it is to be assumed that the shear strength of the discontinuity surfaces can be defined by equations 6 and 7, as discussed in the previous section, then in order to determine the values of ϕ'_i and c'_i for substitution into equation 14, the effective normal stress σ' acting across the discontinuity must be known. This is found from:

$$\sigma' = \frac{1}{2}(\sigma'_1 + \sigma'_3) - \frac{1}{2}(\sigma'_1 - \sigma'_3) \cos 2\beta \quad (15)$$

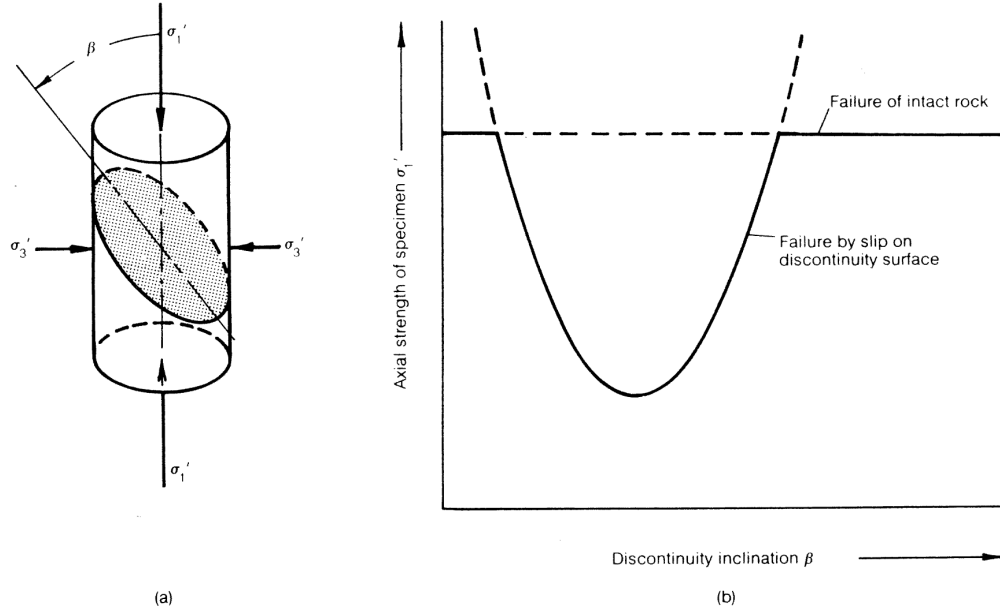


Figure 11 : (a) Configuration of triaxial test specimens containing a pre-existing discontinuity;(b) strength of specimen predicted by means of equations 14 and 15.

However, since σ'_1 is the strength to be determined, the following iterative process can be used:

- Calculate the strength σ'_{1i} of the intact material by means of equation 3, using the appropriate values of σ_c , m and s .
- Determine values of m_j and s_j for the joint (discontinuity) surfaces from direct shear or triaxial test data. Note that the value of σ_c , the unconfined compressive strength, is the same for the intact material and the discontinuity surfaces in this analysis.
- Use the value σ'_{1i} , calculated in step 1, to obtain the first estimate of the effective normal stress σ' from equation 15.
- Calculate τ , ϕ'_i and c'_i from equations 7, 6 and 8, using the value of m_j and s_j from step b, and the value of σ' from step c.
- Calculate the axial strength σ'_{1j} from equation 14.
- If σ'_{1j} is negative or greater than σ'_{1i} , the failure of the intact material occurs in preference to slip on the discontinuity, and the strength of the specimen is defined by equation 3.
- If σ'_{1j} is less than σ'_{1i} then failure occurs as a result of slip on the discontinuity. In this case, return to step c and use the axial strength calculated in step 5 to calculate a new value for the effective normal stress σ' .
- Continue this iteration until the difference between successive values of σ'_{1j} in step e is less than 1%. It will be found that only three or four iterations are required to achieve this level of accuracy.

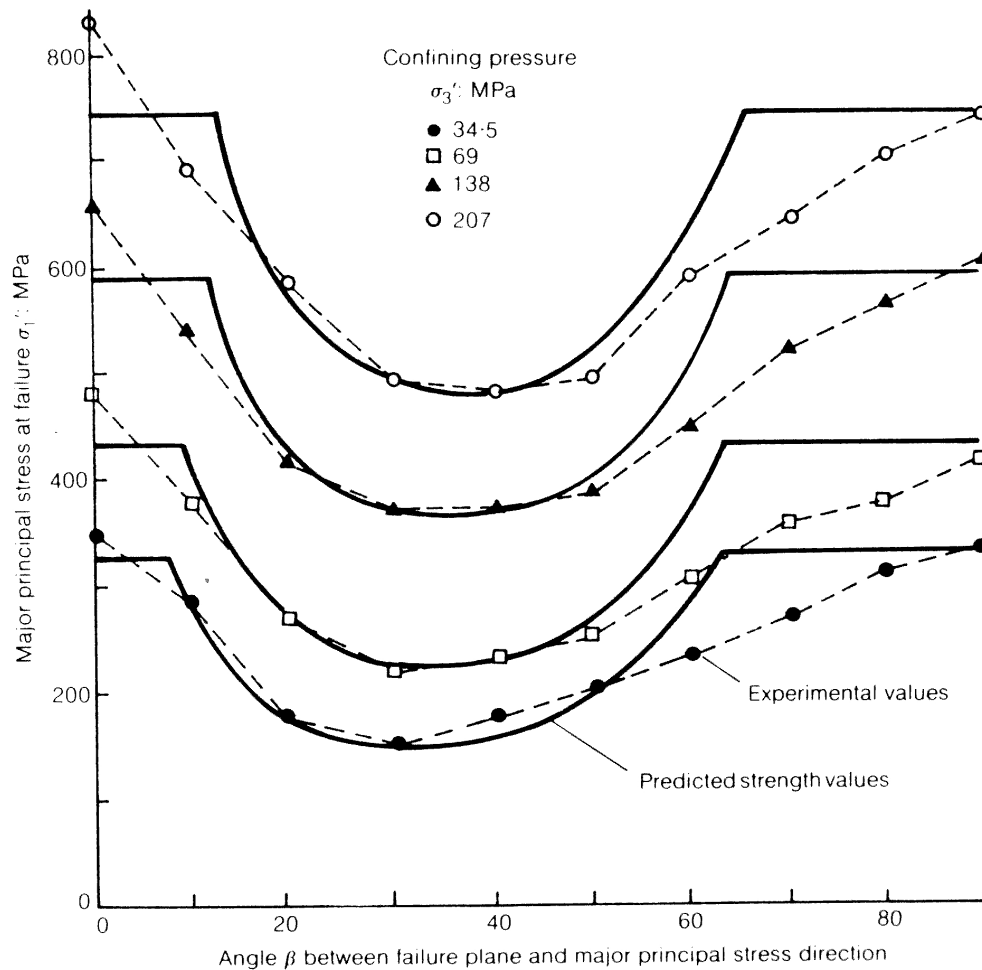


Figure 12 : Triaxial test results for slate with different failure plane inclinations, obtained by McLamore and Gray (1967), compared with strength predictions from equations 3 and 14.

Examples of the analysis described above are given in figures 12 and 13.

The results of triaxial tests on slate tested by McLamore and Gray (1967) for a range of confining pressures and cleavage orientations are plotted in figure 12. The solid curves have been calculated, using the method outlined above, for $\sigma_c = 217$ MPa (unconfined strength of intact rock), $m = 5.25$ and $s = 1.00$ (constants for intact rock), and $m_j = 1.66$ and $s_j = 0.006$ (constants for discontinuity surfaces).

The values of the constants m_j and s_j for the discontinuity surfaces were determined by statistical analysis of the minimum axial strength values, using the procedure for broken rock, described in Appendix 1.

A similar analysis is presented in figure 13, which gives results from triaxial tests on sandstone by Horino and Ellikson (1970). In this case the discontinuity surfaces were created by intentionally fracturing intact sandstone in order to obtain very rough fresh

surfaces. The constants used in plotting the solid curves in figure 13 were $\sigma_c = 177.7$ MPa (intact rock strength), $m = 22.87$ and $s = 1.00$ (constants for intact rock), $m_j = 4.07$ and $s_j = 0$ (constants for induced fracture planes).

The rougher failure surfaces in the sandstone, as compared with the slate (compare values of m_j), give more sudden changes in axial strength with discontinuity inclination. In both of these cases, and in a number of other examples analyzed, the agreement between measured and predicted strengths is adequate for most practical design purposes.

An example of the application of the analysis of anisotropic failure, presented on the preceding pages, is given later. This example involves the determination of the stress distribution and potential failure zones in highly stressed schistose rock surrounding a tunnel.

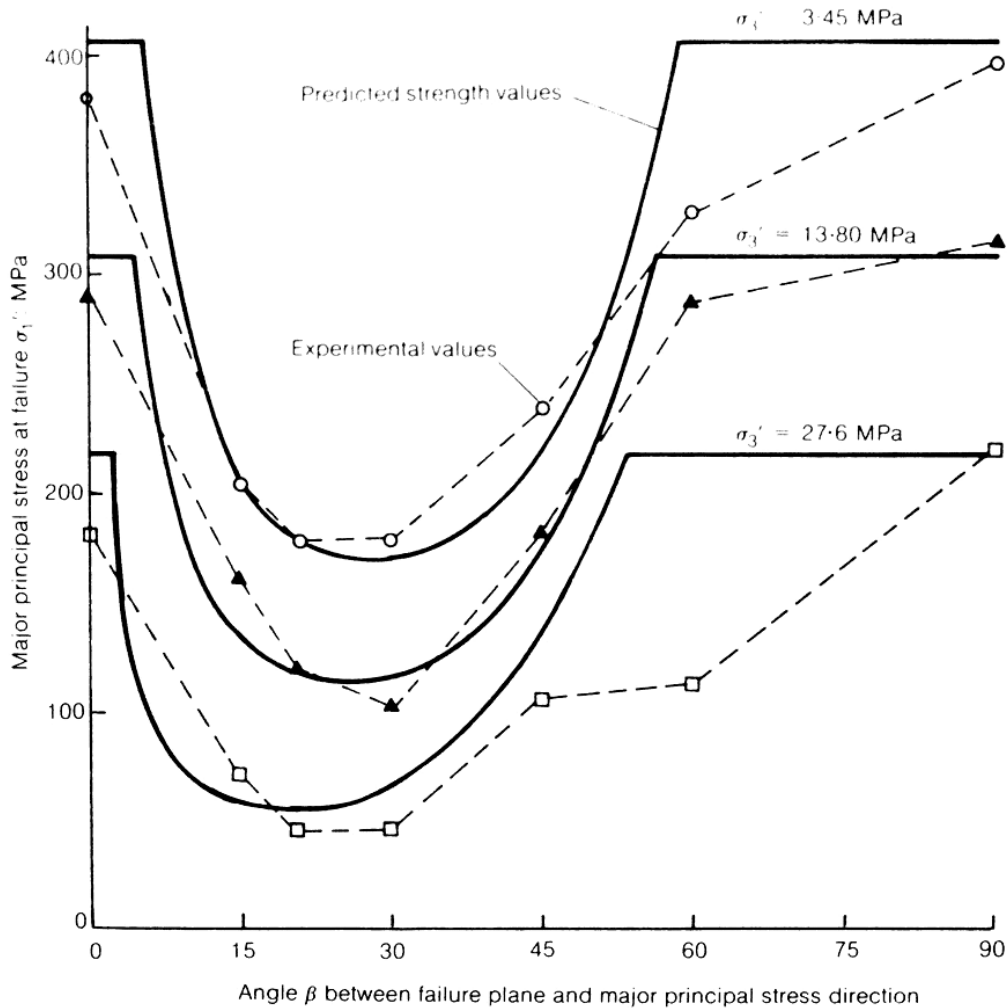


Figure 13 : Triaxial test results for fractured sandstone, tested by Horino and Ellikson (1970), compared with predicted anisotropic strength

Failure of jointed rock masses

Having studied the strength of intact rock and of discontinuities in rock, the next logical step is to attempt to predict the behaviour of a jointed rock mass containing several sets of discontinuities. The simplest approach to this problem is to superimpose a number of analyses for individual discontinuity sets, such as those presented in figures 12 and 13, in the hope that the overall behaviour pattern obtained would be representative of the behaviour of an actual jointed rock mass.

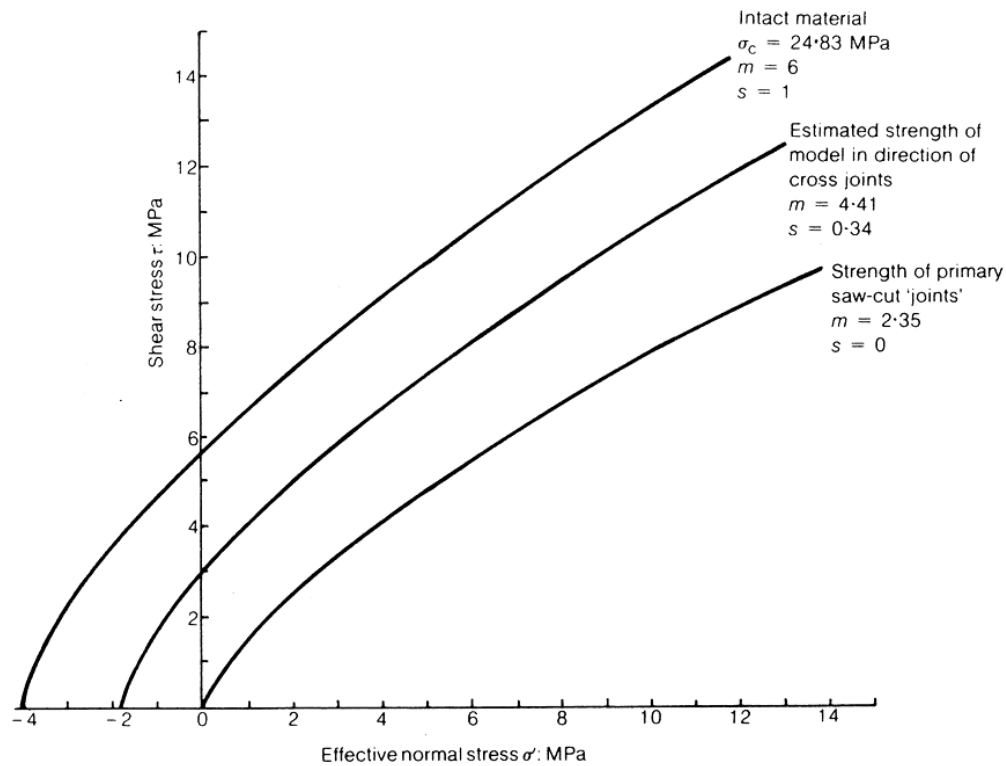


Figure 14 : Mohr failure envelopes for brickwall model tested by Ladanyi and Archambault (1972)

Verification of the results of such predictions presents very complex experimental problems, and many research workers have resorted to the use of physical models in an attempt to minimize these experimental difficulties. Lama and Vutukuri (1978) have presented a useful summary of the results of model studies carried out by John (1962), Muller and Packer (1965), Lajtai (1967), Einstein et al (1969), Ladanyi and Archambault (1970, 1972), Brown (1970), Brown and Trollope (1970), Walker (1971) and others. One of these studies, published by Ladanyi and Archambault (1972), will be considered here.

Ladanyi and Archambault constructed models from rods, with a square cross-section of 12.7 mm and a length of 63.5 mm, which had been sawn from commercial compressed concrete bricks. The Mohr failure envelopes for the intact concrete material and for the sawn 'joints' in the model are given in figure 14. These curves were derived by statistical analysis of raw test data supplied to the author by Professor B. Ladanyi.

One of the model configurations used by Ladanyi and Archambault (1972) is illustrated in figure 15. As will be seen from this drawing, failure of the model in the direction of the 'cross joints' (inclined at an angle α to the major principal stress direction) would involve fracture of intact material as well as sliding on the joints. A crude first approximation of the model strength in the α direction is obtained by simple averaging of the Mohr failure envelopes for the intact material and the through-going joints. The resulting strength estimate is plotted as a Mohr envelope in figure 14.

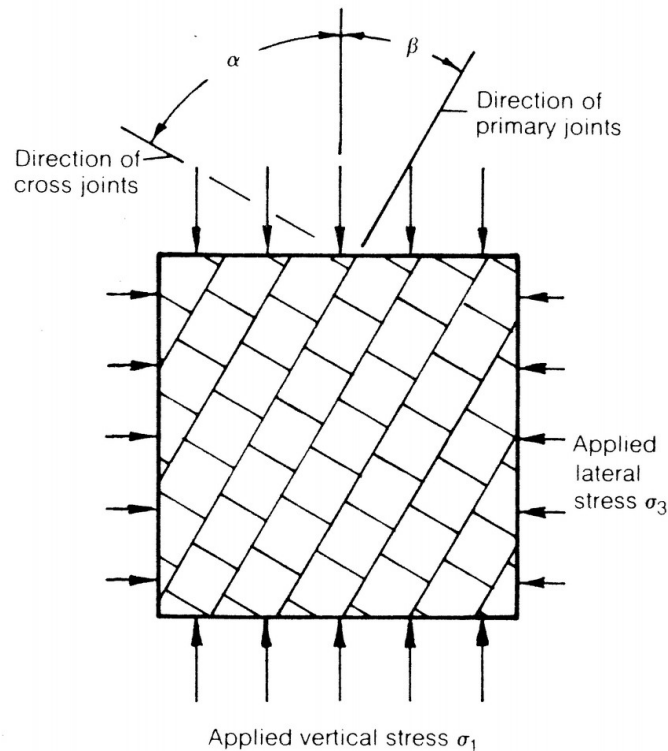


Figure 15 : Configuration of brickwall model tested by Ladanyi and Archambault (1972)

The predicted strength behaviour of Ladanyi and Archambault's 'brickwall' model, for different joint orientations and lateral stress levels, is given in figure 16a. These curves have been calculated, from the strength values given in figure 14, by means of equations 14, 15 and 3, as discussed in the previous section. The actual strength values measured by Ladanyi and Archambault are plotted in figure 16b. Comparison between these two figures leads to the following conclusions:

1. There is an overall similarity between predicted and observed strength behaviour which suggests that the approach adopted in deriving the curves plotted in figure 16a is not entirely inappropriate.
2. The observed strengths are generally lower than the predicted strengths. The intact material strength is not achieved, even at the most favourable joint

orientations. The sharply defined transitions between different failure modes, predicted in figure 16a, are smoothed out by rotation and crushing of individual blocks. This behaviour is illustrated in the series of photographs reproduced in figure 17. In particular, the formation of 'kink bands', as illustrated in figure 17c, imparts a great deal of mobility to the model and results in a significant strength reduction in the zone defined by $15^\circ > \alpha > 45^\circ$, as shown in figure 16b.

3. Intuitive reasoning suggests that the degree of interlocking of the model blocks is of major significance in the behaviour of the model since this will control the freedom of the blocks to rotate. In other words, the freedom of a rock mass to dilate will depend upon the interlocking of individual pieces of rock which, in turn, will depend upon the particle shape and degree of disturbance to which the mass has been subjected. This reasoning is supported by experience in strength determination of rock fill where particle strength and shape, particle size distribution and degree of compaction are all important factors in the overall strength behaviour.
4. Extension of the principle of strength prediction used in deriving the curves presented in figure 16a to rock masses containing three, four or five sets of discontinuities, suggests that the behaviour of such rock masses would approximate to that of a homogeneous isotropic system. In practical terms, this means that, for most rock masses containing a number of joint sets with similar strength characteristics, the overall strength behaviour will be similar to that of a very tightly interlocking rock fill.

The importance of the degree of interlocking between particles in a homogeneous rock mass can be illustrated by considering the results of an ingenious experiment carried out by Rosengren and Jaeger (1968), and repeated by Gerogiannopoulos (1979). By heating specimens of coarse grained marble to about 600°C, the cementing material between grains is fractured by different thermal expansion of the grains themselves. The material produced by this process is a very low porosity assemblage of extremely tightly interlocking but independent grains. This 'granulated' marble was tested by Rosengren and Jaeger (1969) and Gerogiannopoulos (1979) in an attempt to simulate the behaviour of an undisturbed jointed rock mass.

The results obtained by Gerogiannopoulos from triaxial tests on both intact and granulated Carrara marble are plotted in figure 18. In order to avoid confusion, Mohr failure circles for the granulated material only are included in this figure. However, statistical analyses of the data sets for both intact and granulated material to obtain σ_c , m and s values gave correlation coefficients in excess of 90%.

Figure 18 shows that the strength difference between intact material and a very tightly interlocking assemblage of particles of the same material is relatively small. It is unlikely that this degree of interlocking would exist in an in situ rock mass, except in very massive rock at considerable depth below surface. Consequently, the Mohr failure envelope for granulated marble, presented in figure 18, represents the absolute upper bound for jointed rock mass strength.

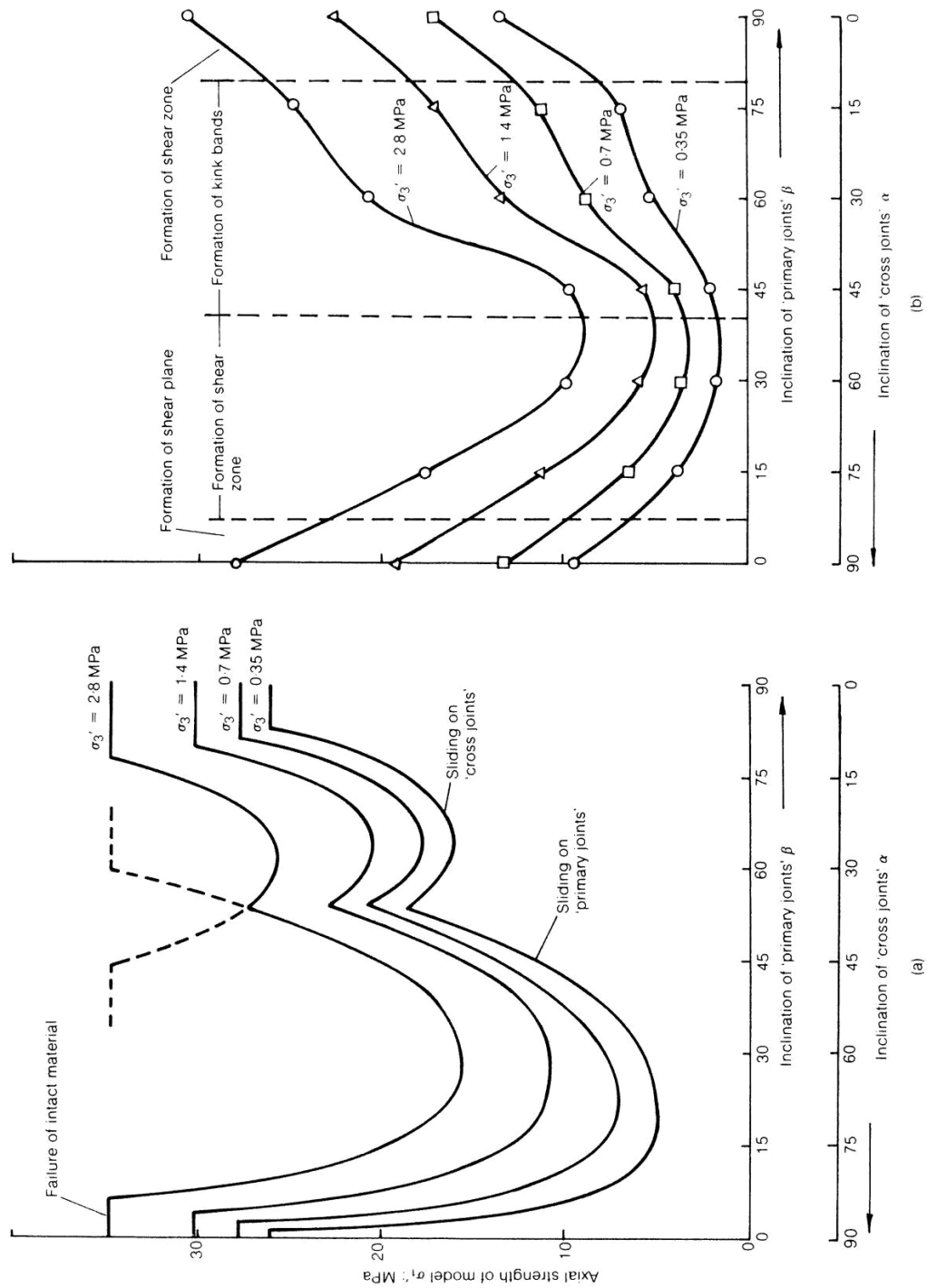


Figure 16. Comparison between a) predicted and b) observed strength of brickwall model tested by Ladanyi & Archambault (1972).

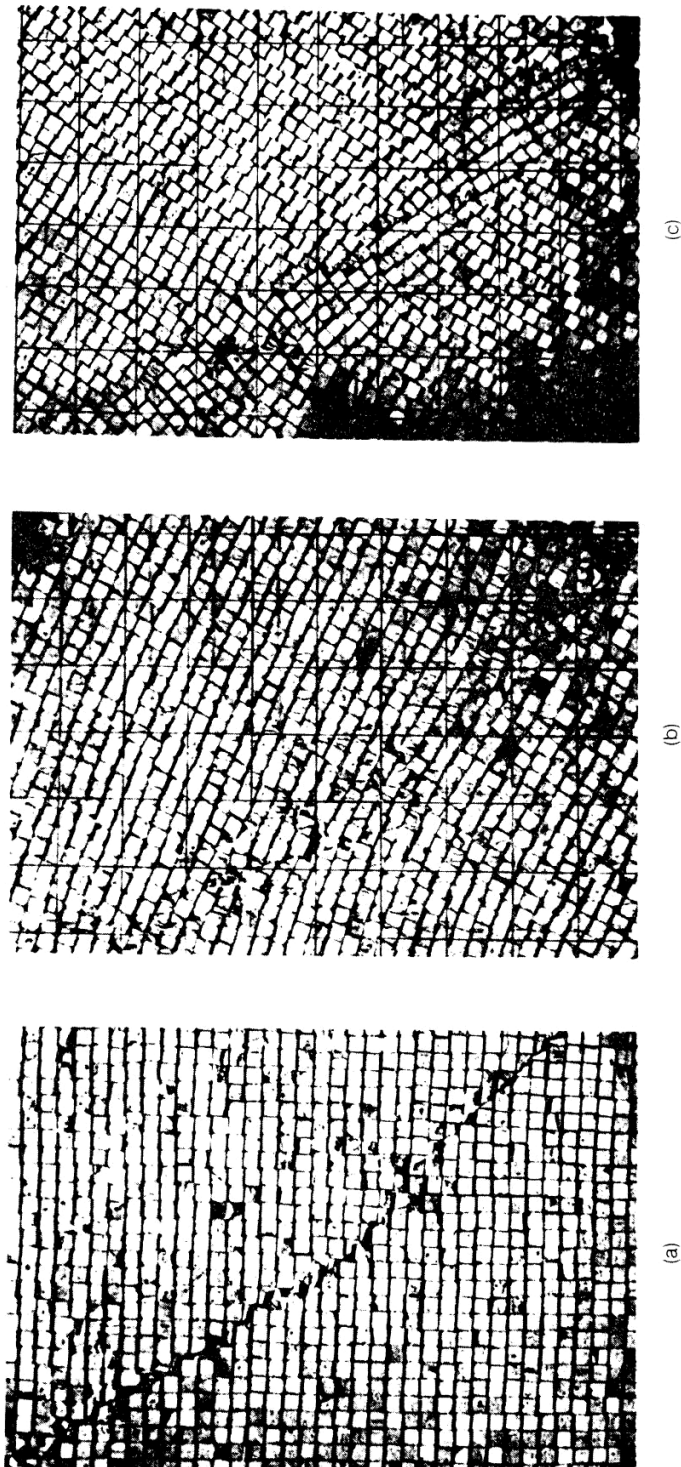


Figure 17. (a) Shear plane failure; (b) shear zone failure; and (c) kink band failure observed in concrete brick models tested by Ladanyi & Archambault (1972). Photograph reproduced with the permission of Professor B. Ladanyi.

Strength of jointed rock masses

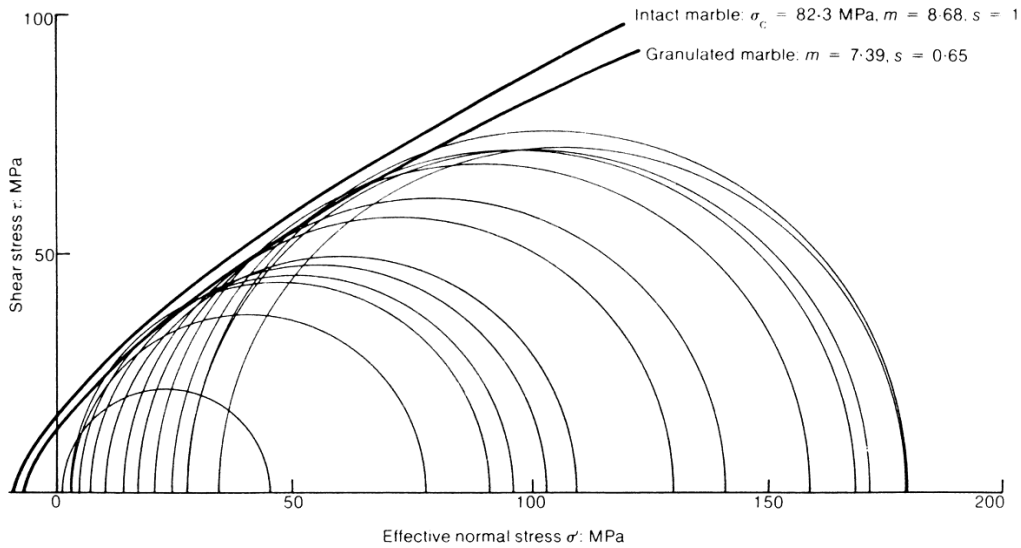


Figure 18 : Comparison between the strength of intact and granulated Carrara marble tested by Gerogiannopoulos (1979).

A more realistic assessment of the strength of heavily jointed rock masses can be made on the basis of triaxial test data obtained in connection with the design of the slopes for the Bougainville open pit copper mine in Papua New Guinea. The results of some of these tests, carried out by Jaeger (1970), the Snowy Mountain Engineering Corporation and in mine laboratories, have been summarized by Hoek and Brown (1980a).

The results of tests on Panguna Andesite are plotted as Mohr envelopes in figure 19. Figure 19a has been included to show the large strength difference between the intact material and the jointed rock mass. Figure 19b is a 100X enlargement of the low stress portion of figure 19a, and gives details of the test results on the jointed material. Details of the materials tested are given in table 3.

Particular mention must be made of the 'undisturbed' 152 mm diameter core samples of jointed Panguna Andesite tested by Jaeger (1970). These samples were obtained by very careful triple-tube diamond core drilling in an exploration adit in the mine. The samples were shipped to Professor Jaeger's laboratory in Canberra, Australia, in the inner tubes of the core barrels, and then carefully transferred onto thin copper sheets which were soldered to form containers for the specimens. These specimens were rubber sheathed and tested triaxially. This series of tests is, as far as the author is aware, the most reliable set of tests ever carried out on 'undisturbed' jointed rock.

The entire Bougainville testing programme, with which the author has been associated as a consultant since its inception, extended over a ten year period and cost several hundred thousand pounds. This level of effort was justified because of the very large economic and safety considerations involved in designing a final slope of almost 1000 m high for one side of the open pit. Unfortunately, it is seldom possible to justify testing programmes of this magnitude in either mining or civil engineering projects, and hence the results summarized in figure 19 represent a very large proportion of the sum total of all published data on this subject.

Strength of jointed rock masses

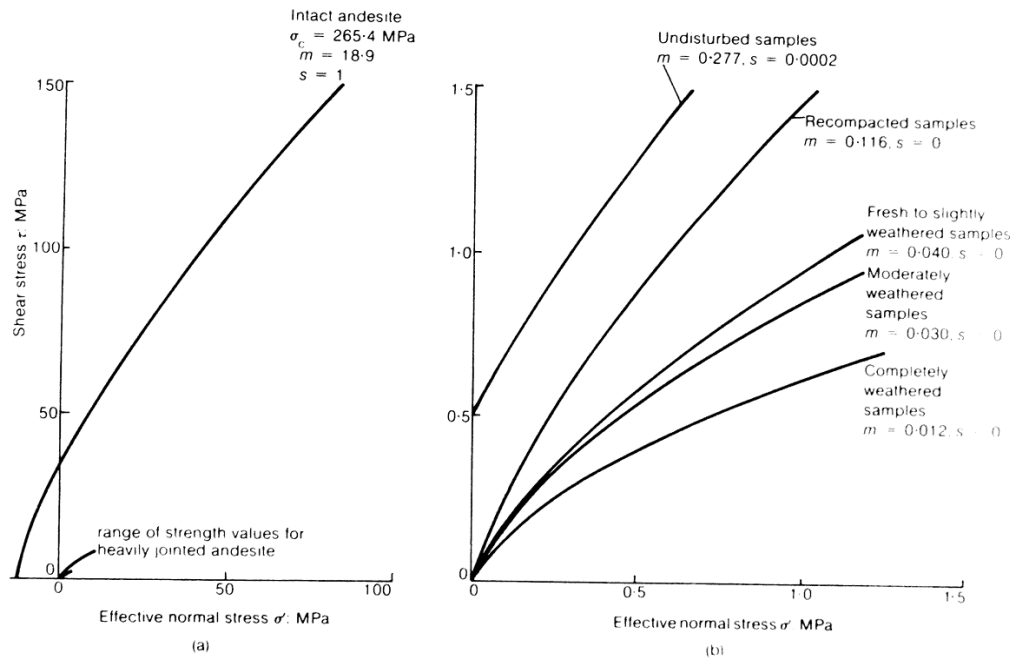


Figure 19 : Mohr failure envelopes for (a) intact and (b) heavily jointed Panguna andesite from Bougainville, Papua New Guinea (see Table 3 for description of materials).

Table 3. Details of materials and test procedures for Panguna andesite.

Material	Tested by	Sample diameter: mm	Material constants
Intact Panguna andesite	Jaeger (1970) Golder Associates	25 50	$\sigma_c = 265.4$ MPa $m = 18.9$ $s = 1$ Correlation coefficient 0.85
Undisturbed core samples of heavily jointed andesite obtained by triple-tube diamond core drilling in exploration adit	Jaeger (1970)	152	$m = 0.277$ $s = 0.0002$ Correlation coefficient 0.99
Recompacted sample of heavily jointed andesite collected from mine benches (equivalent to compacted fresh rock-fill)	Bougainville Copper	152	$m = 0.116$ $s = 0$
Fresh to slightly weathered andesite, lightly recompacted	Snowy Mountains Engineering Corporation	570	$m = 0.040$ $s = 0$
Moderately weathered andesite, lightly recompacted	Snowy Mountains Engineering Corporation	570	$m = 0.030$ $s = 0$
Completely weathered andesite (equivalent to poor quality waste rock)	Snowy Mountains Engineering Corporation	570	$m = 0.012$ $s = 0$

A similar, although less ambitious, series of tests was carried out on a highly fractured greywacke sandstone by Raphael and Goodman (1979). The results of these tests, plotted in figure 20, show a much lower reduction from intact to jointed rock mass strength than for the Panguna Andesite (figure 19). This is presumably because the intact sandstone tested by Raphael and Goodman is significantly weaker than the andesite tested by Jaeger, and hence there is less possibility of the block rotation mechanism (see figure 17c) which appears to contribute so much to the weakness of jointed systems in strong materials. The author freely admits that this suggestion is highly speculative, and is based upon intuitive reasoning rather than experimental facts.

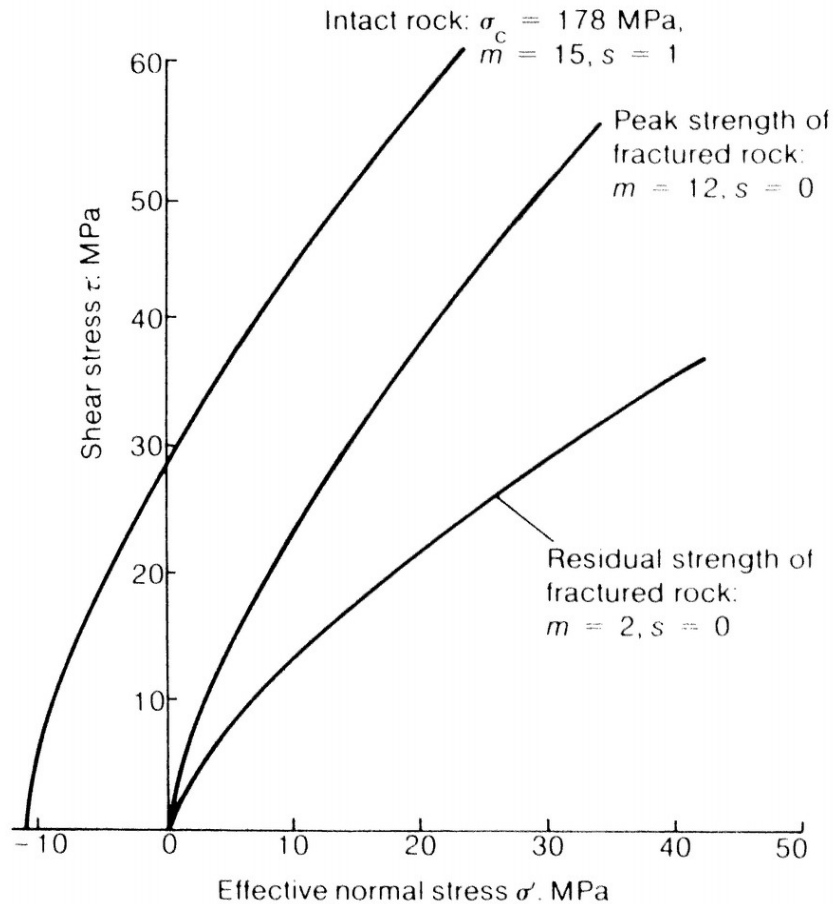


Figure 20 : Mohr failure envelopes estimated from plotted triaxial test data (Raphael and Goodman, 1979) for highly fractured, fresh to slightly altered greywacke sandstone.

Estimating the strength of jointed rock

Based on their analyses of the results from tests on models, jointed rock masses and rock fill, Hoek and Brown (1980b) proposed an approximate method for estimating the strength of jointed rock masses. This method, summarized in Table 4, involves estimating the values of the empirical constants m and s from a description of the rock mass. These estimates, together with an estimate of the uniaxial compressive strength

of the intact pieces of rock, can then be used to construct an approximate Mohr failure envelope for the jointed rock mass.

As a means of assisting the user in describing the rock mass, use is made of the rock mass classification systems proposed by Bieniawski (1974) and Barton et al (1974). Space does not permit a review of these classification systems, and hence the reader is referred to the original papers or to the extensive summary published by Hoek and Brown (1980a).

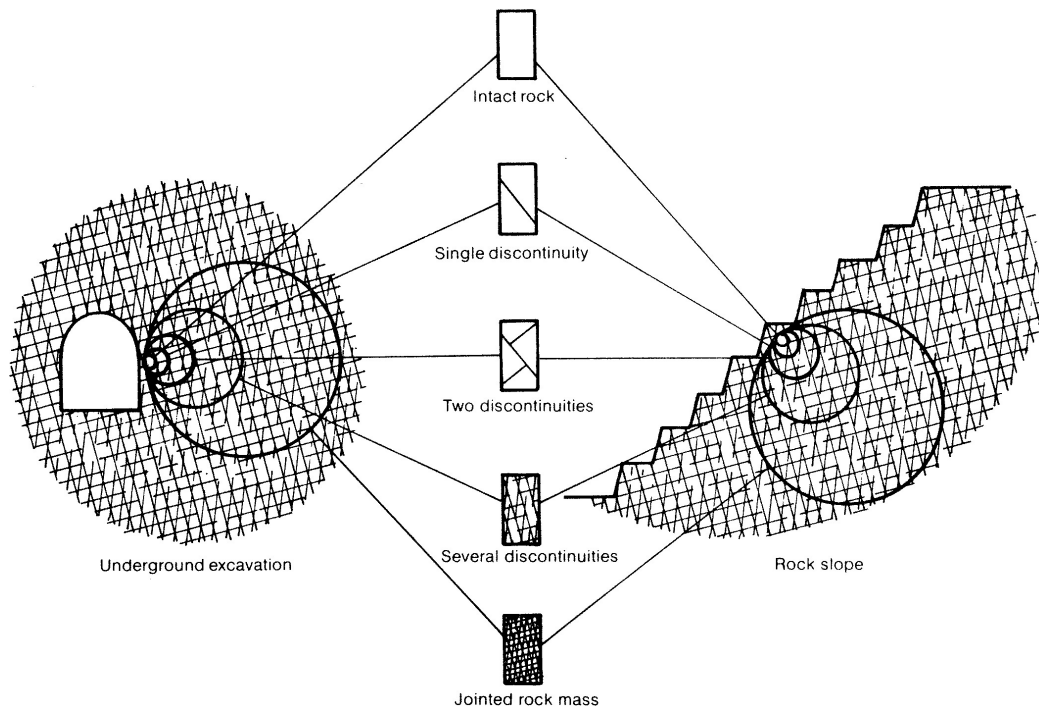


Figure 21 : Simplified representation of the influence of scale on the type of rock mass behaviour model which should be used in designing underground excavations or rock slopes.

The author's experience in using the values listed in Table 4 for practical engineering design suggests that they are somewhat conservative. In other words, the actual rock mass strength is higher than that estimated from the Mohr envelopes plotted from the values listed. It is very difficult to estimate the extent to which the predicted strengths are too low, since reliable field data are almost non-existent. However, based on comparisons between observed and predicted behaviour of rock slopes and underground excavations, the author tends to regard the strength estimates made from Table 4 as lower bound values for design purposes. (For further discussion on this question, see the addendum at the end of this paper). Obviously, in designing an important structure, the user would be well advised to obtain his own test data before deciding to use strength values significantly higher than those given in Table 4.

Table 4. Approximate relationship between rock mass quality and material constants.

Empirical failure criterion $\sigma_1' = \sigma_3' + (m\sigma_c \sigma_3' + s\sigma_c^2)^{1/2}$ σ_1' = major principal stress σ_3' = minor principal stress σ_c = uniaxial compressive strength of intact rock m, s = empirical constants	Carbonate rocks with well developed crystal cleavage, e.g. dolomite, limestone and marble	Lithified argillaceous rocks, e.g. mudstone, siltstone, shale and slate (tested normal to cleavage)	Arenaceous rocks with strong crystals and poorly developed crystal cleavage, e.g. sandstone and quartzite	Fine grained polyminerallitic igneous crystalline rocks, e.g. andesite, dolerite, diabase and rhyolite	Coarse grained polyminerallitic igneous and metamorphic crystalline rocks, e.g. amphibolite, gabbro, gneiss, granite, norite and quartzdiorite
Intact rock samples Laboratory size samples free from pre-existing fractures Bieniawski, 1974b (CSIR)* rating 100 Barton <i>et al.</i> , 1974 (NGI)† rating 500	$m = 7$ $s = 1$	$m = 10$ $s = 1$	$m = 15$ $s = 1$	$m = 17$ $s = 1$	$m = 25$ $s = 1$
Very good quality rock mass Tightly interlocking undisturbed rock with rough unweathered joints spaced at 1 to 3 m Bieniawski, 1974b (CSIR) rating 85 Barton <i>et al.</i> , 1974 (NGI) rating 100	$m = 3.5$ $s = 0.1$	$m = 5$ $s = 0.1$	$m = 7.5$ $s = 0.1$	$m = 8.5$ $s = 0.1$	$m = 12.5$ $s = 0.1$
Good quality rock mass Fresh to slightly weathered rock, slightly disturbed with joints spaced at 1 to 3 m Bieniawski, 1974b (CSIR) rating 65 Barton <i>et al.</i> , 1974 (NGI) rating 10	$m = 0.7$ $s = 0.004$	$m = 1$ $s = 0.004$	$m = 1.5$ $s = 0.004$	$m = 1.7$ $s = 0.004$	$m = 2.5$ $s = 0.004$
Fair quality rock mass Several sets of moderately weathered joints spaced at 0.3 to 1 m, disturbed Bieniawski, 1974b (CSIR) rating 44 Barton <i>et al.</i> , 1974 (NGI) rating 1	$m = 0.14$ $s = 0.0001$	$m = 0.20$ $s = 0.0001$	$m = 0.30$ $s = 0.0001$	$m = 0.34$ $s = 0.0001$	$m = 0.50$ $s = 0.0001$
Poor quality rock mass Numerous weathered joints at 30 to 500 mm with some gouge. Clean, compacted rockfill Bieniawski, 1974b (CSIR) rating 23 Barton <i>et al.</i> , 1974 (NGI) rating 0.1	$m = 0.04$ $s = 0.00001$	$m = 0.05$ $s = 0.00001$	$m = 0.08$ $s = 0.00001$	$m = 0.09$ $s = 0.00001$	$m = 0.13$ $s = 0.00001$
Very poor quality rock mass Numerous heavily weathered joints spaced at 50 mm with gouge. Waste rock Bieniawski, 1974b (CSIR) rating 3 Barton <i>et al.</i> , 1974 (NGI) rating 0.01	$m = 0.007$ $s = 0$	$m = 0.010$ $s = 0$	$m = 0.015$ $s = 0$	$m = 0.017$ $s = 0$	$m = 0.025$ $s = 0$

* CSIR Commonwealth Scientific and Industrial Research Organization.

† NGI Norway Geotechnical Institute.

In order to use table 4 to make estimates of rock mass strength, the following steps are suggested :

- (a) From a geological description of the rock mass, and from a comparison between the size of the structure being designed and the spacing of discontinuities in the rock mass (see figure 21), decide which type of material behaviour model is most appropriate. The values listed in table 4 should only be used for estimating the strength of intact rock or of heavily jointed rock masses containing several sets of discontinuities of similar type. For schistose rock or for jointed rock masses containing dominant discontinuities such as faults, the

behaviour will be anisotropic and the strength should be dealt with in the manner described in example 1.

- (b) Estimate the unconfined compressive strength σ_c of the intact rock pieces from laboratory test data, index values or descriptions of rock hardness (see Hoek and Bray (1981) or Hoek and Brown (1980a)). This strength estimate is important since it establishes the scale of the Mohr failure envelope.
- (c) From a description of the rock mass or, preferably, from a rock mass classification using Barton et al (1974) or Bieniawski's (1974) system, determine the appropriate row and column in table 4, or calculate m and s values from equations 17 to 20.
- (d) Using equations 6 and 7, calculate and plot a Mohr failure envelope for the estimated values of σ_c , m and s . Draw an approximate average Mohr Coulomb linear envelope through the plotted points, and estimate the average friction angle and cohesive strength of the rock mass. Compare these values with published data for rock fill (Marachi, Chan and Seed (1972); Marsal (1967, 1973); Charles and Watts (1980)) or with data given in this paper to ensure that the values are reasonable.
- (e) Use the estimated strength values for preliminary design purposes and carry out sensitivity studies by varying the values of m and s to determine the importance of rock mass strength in the design.
- (f) For critical designs which are found to be very sensitive to variations in rock mass strength, establish a site investigation and laboratory testing programme aimed at refining the strength estimates made on the basis of the procedure outlined in the preceding steps.

Examples of application of rock mass strength estimates in engineering design

In order to illustrate the application of the empirical failure criterion presented to practical engineering design problems, three examples are given. These examples have been carefully chosen to illustrate particular points and, although all of the examples are hypothetical, they are based upon actual engineering problems studied by the author.

Example 1

Figure 22 gives a set of contours of the ratio of available strength to induced stress in a schistose gneiss rock mass surrounding a tunnel. The following assumptions were made in calculating these ratios.

The vertical in situ stress in the rock surrounding the tunnel is 40 MPa, corresponding to a depth below surface of about 1500m. The horizontal in situ stress is 60 MPa or 1.5 times the vertical stress.

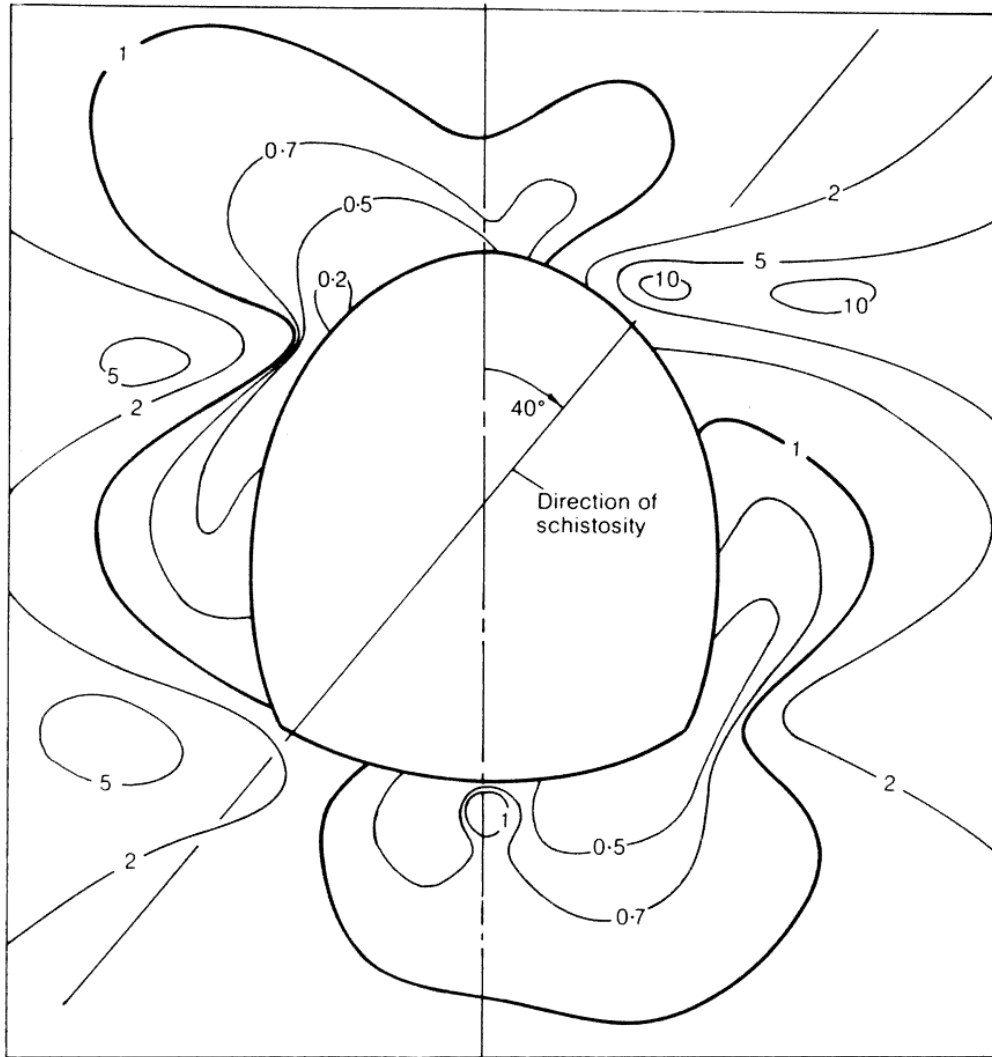


Figure 22 : Contours of ratio of available strength to stress in schistose rock surrounding a highly stressed tunnel.

The rock strength is defined by the following constants: uniaxial compressive strength of intact rock $\sigma_c = 150$ MPa, material constants for the isotropic rock mass: $m_i = 12.5$, $s_i = 0.1$, material constants for joint strength in the direction of schistosity: $m_j = 0.28$, $s_j = 0.0001$.

The direction of schistosity is assumed to be at 40° (measured in a clockwise direction) to the vertical axis of the tunnel.

The rock mass surrounding the tunnel is assumed to be elastic and isotropic. This assumption is generally accurate enough for most practical purposes, provided that the ratio of elastic moduli parallel to and normal to schistosity does not exceed three. In the case of the example illustrated in figure 22, the stress distribution was calculated by means of the two-dimensional boundary element stress analysis technique, using

the programming listing published by Hoek and Brown (1980a). A modulus of elasticity of $E = 70$ GPa and a Poisson's ratio of $\nu = 0.25$ were assumed for this analysis.

The shear and normal stresses τ and σ' , acting on a plane inclined at 40° (clockwise) to the vertical axis, were calculated for each point on a grid surrounding the tunnel. The available shear strengths in the direction of this plane, τ_{as} , were calculated by means of equations 7 and 6 for $\sigma_c = 150$ MPa, $m_j = 0.28$ and $s_j = 0.0001$. Hence, the ratio of available shear strength τ_{as} to the induced shear stress τ was determined for each grid point.

In addition, the available strength σ'_{ai} of the isotropic rock mass was calculated for each grid point by means of equation 3, using the principal stresses σ'_1 and σ'_3 and the isotropic rock mass material properties ($\sigma_c = 150$ MPa, $m_i = 12.5$ and $s_i = 0.1$). This available strength σ'_{ai} was compared with the induced maximum principal stress σ'_1 to obtain the ratio σ'_{ai}/σ'_1 at each grid point.

In plotting the contours illustrated in figure 22, the lower of the two ratios τ_{as}/τ and σ'_{ai}/σ'_1 was used to define the strength to stress ratio value.

The zones surrounded by the contours defined by a strength to stress ratio of one contain overstressed rock. The general method used in designing tunnels and caverns in highly stressed rock is to attempt to minimize the extent of such overstressed zones by choice of the excavation shape and orientation in relation to the in situ stress direction.

When zones of overstressed rock, such as those illustrated in figure 22, are unavoidable, appropriate support systems have to be designed in order to restrict the propagation of fracture of rock contained in these zones. Unfortunately, the analysis presented in this example cannot be used to predict the extent and direction of fracture propagation from the zones of overstressed rock and the choice of support systems tends to be based upon very crude approximations.

Such approximations involve designing a system of rockbolts with sufficient capacity to support the weight of the rock contained in the overhead overstressed zones and of sufficient length to permit anchoring in the rock outside these zones.

Improved techniques for support design are being developed, but are not yet generally available for complex failure patterns such as that illustrated in figure 22. These techniques, discussed by Hoek and Brown (1980a), involve an analysis of the interaction between displacements, induced by fracturing in the rock surrounding the tunnel, and the response of the support system installed to control these displacements. It is hoped that these support-interaction analyses will eventually be developed to the point where they can be used to evaluate the support requirements for tunnels such as that considered in this example.

Example 2

This example involves a study of the stability of a very large rock slope such as that

Strength of jointed rock masses

which would be excavated in an open pit mine. The benched profile of such a slope, having an overall angle of about 30° and a vertical height of 400m, is shown in figure 23.

The upper portion of the slope is in overburden material comprising mixed sands, gravels and clays. Back-analysis of previous failures in this overburden material, assuming a linear Mohr failure envelope, gives a friction angle of $\phi' = 18^\circ$ and a cohesive strength $c' = 0$. The unit weight of this material averages 0.019 MN/m^3 .

The overburden is separated from the shale forming the lower part of the slope by a fault which is assumed to have a shear strength defined by $\phi' = 15^\circ$ and $c' = 0$.

No strength data are available for the shale, but examination of the rock exposed in tunnels in this material suggests that the rock mass can be rated as 'good quality'. From Table 4, the material constants $m = 1$ and $s = 0.004$ are chosen as representative of this rock. In order to provide a measure of conservatism in the design, the value of s is downgraded to zero to allow for the influence of stress relaxation which may occur as the slope is excavated. The strength of the intact material is estimated from point load tests (see Hoek and Brown, 1980a) as 30 MPa. The unit weight of the shale is 0.023 MN/m^3 .

The phreatic surface in the rock mass forming the slope, shown in figure 23, is estimated from a general knowledge of the hydrogeology of the site and from observations of seepage in tunnels in the slope.

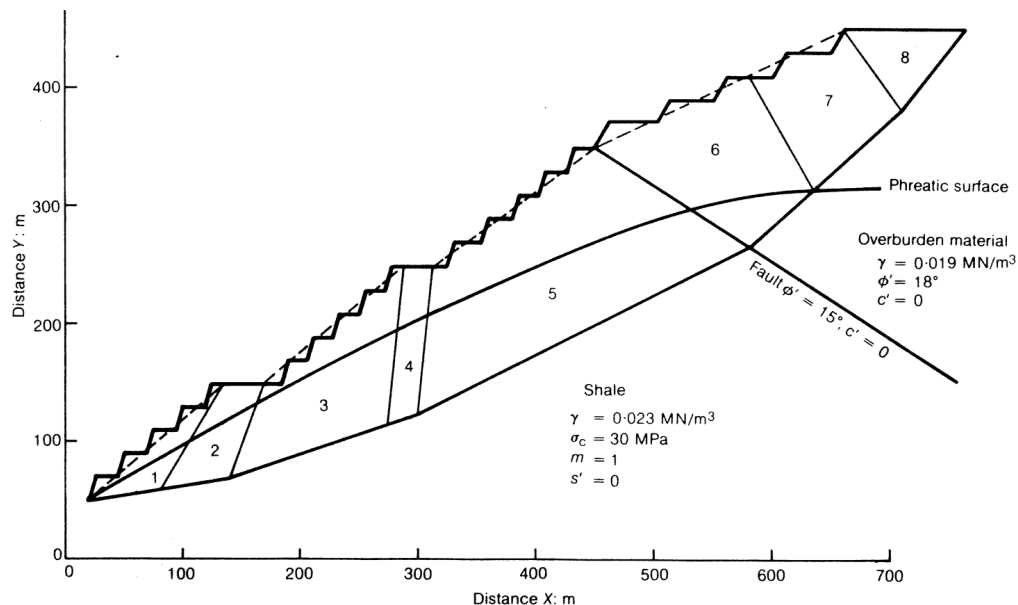


Figure 23 : Rock slope analysed in example 2 (see Table 5 for coordinates of slope profile, phreatic surface and failure surface).

Strength of jointed rock masses

Analysis of the stability of this slope is carried out by means of the non-vertical slice method (Sarma, 1979). This method is ideally suited to many rock slope problems because it permits the incorporation of specific structural features such as the fault illustrated in figure 23.

Sarma's analysis has been slightly modified by this author and programmed for use on a micro-computer (Hoek, 1986).

Table 5: Stability analysis of slope shown in Fig. 23.

Slice	1	2	3	4	5	6	7	8	9
XT	20	135	170	288	312	450	580	660	765
YT	50	150	150	250	250	350	410	450	450
XW	20	106	162	284	308	530	635	710	765
YW	50	100	132	196	210	300	311	380	450
XB	20	82	140	274	300	580	635	710	765
YB	50	60	68	115	123	265	311	380	450
Unit weight γ : MN/m ³	0.023	0.023	0.023	0.023	0.023	0.019	0.019	0.019	Factor of safety
First iteration									
ϕ'_B	30	30	30	30	30	18	18	18	1.69
c'_B	1.0	1.0	1.0	1.0	1.0	0	0	0	
ϕ'_S	0	30	30	30	30	15	18	18	
c'_S	0	1.0	1.0	1.0	1.0	0	0	0	
σ'_B	1.32	0.77	1.40	1.57	1.89	0.58	1.38	0.54	
σ'_S	0	0.09	0.55	0.66	0.75	2.01	1.21	0.52	
Second iteration									
ϕ'_B	40.03	45.08	39.46	38.36	36.58	18	18	18	1.57
c'_B	0.48	0.32	0.51	0.55	0.64	0	0	0	
ϕ'_S	0	62.08	48.11	46.48	45.32	15	18	18	
c'_S	0	0.06	0.25	0.28	0.31	0	0	0	
σ'_B	0.74	1.07	1.31	1.76	1.96	0.57	1.37	0.53	
σ'_S	0	0.16	0.46	0.53	0.62	2.00	1.19	0.51	
Third iteration									
ϕ'_B	45.44	42.02	40.10	37.26	36.23	18	18	18	1.57
c'_B	0.31	0.41	0.48	0.61	0.66	0	0	0	
ϕ'_S	0	58.10	49.67	48.44	47.04	15	18	18	
c'_S	0	0.10	0.21	0.24	0.27	0	0	0	
σ'_B	0.74	1.07	1.31	1.76	1.96	0.57	1.37	0.53	
σ'_S	0	0.15	0.44	0.52	0.61	2.00	1.19	0.51	

Table 5 lists the coordinates of the slope profile (XT, YT), the phreatic surface (XW, YW), and the base or failure surface (YB, YB) which was found, from a number of analyses, to give the lowest factor of safety. As a first approximation, the strength of the shale is assumed to be defined by $\phi' = 30^\circ$ and $c' = 1$ MPa. Analysis of the slope, using these values, gives a factor of safety of 1.69.

The effective normal stresses σ'_B and σ'_S on the slice bases and sides, respectively, are calculated during the course of this analysis and these values are listed, for each slice, in Table 5. These values are used to determine the appropriate values for the instantaneous friction angle ϕ'_i and the instantaneous cohesive strength c'_i for the shale by means of equations 6 and 7 (for $\sigma_c = 30$ MPa, $m = 1$ and $s = 0$). These values of ϕ'_i and c'_i are used in the second iteration of a stability analysis and, as shown in Table 5, the resulting factor of safety is 1.57.

This process is repeated a third time, using the values of ϕ'_i and c'_i calculated from the effective normal stresses given by the second iteration. The factor of safety given by the third iteration is 1.57. An additional iteration, not included in Table 5, gave the same factor of safety and no further iterations were necessary.

This example is typical of the type of analysis which would be carried out during the feasibility or the basic design phase of a large open pit mine or excavation for a dam foundation or spillway. Further analyses of this type would normally be carried out at various stages during excavation of the slope as the rock mass is exposed and more reliable information becomes available. In some cases, a testing programme may be set up to attempt to investigate the properties of materials such as the shale forming the base of the slope shown in figure 23.

Example 3

A problem which frequently arises in both mining and civil engineering projects is that of the stability of waste dumps on sloping foundations. This problem has been studied extensively by the Commonwealth Scientific and Industrial Research Organization in Australia in relation to spoil pile failures in open cast coal mines (see, for example, Coulthard, 1979). These studies have shown that many of these failures involve the same active-passive wedge failure process analysed by Seed and Sultan (1967, 1969) and Horn and Hendron (1968) for the evaluation of dams with sloping clay cores.

In considering similar problems, the author has found that the non-vertical slice method published by Sarma (1979) and Hoek (1986) is well suited to an analysis of this active-passive wedge failure. Identical results to those obtained by Coulthard (1979) are given by assuming a drained spoil pile with a purely frictional shear strength on the interface between the active and passive wedges. However, Sarma's method allows the analysis of a material with non-linear failure characteristics and, if necessary, with ground water pressures in the pile.

The example considered here involves a 75m high spoil pile with a horizontal upper surface and a face angle of 35°. The unit weight of the spoil material is 0.015 MN/m³. This pile rests on a weak foundation inclined at 12° to the horizontal. The shear strength of the foundation surface is defined by a friction angle of $\phi' = 15^\circ$ and zero cohesion. The pile is assumed to be fully drained.

Triaxial tests on retorted oil shale material forming the spoil pile give the Mohr circles plotted in figure 24. Regression analysis of the triaxial test data, assuming a linear Mohr failure envelope, give $\phi' = 29.5^\circ$ and $c' = 0.205$ MPa with a correlation coefficient to 1.00. Analysis of the same data, using the 'broken rock' analysis given in appendix 1, for $\sigma_c = 25$ MPa (determined by point load testing) gave $m = 0.243$ and $s = 0$. Both linear and non-linear Mohr failure envelopes are plotted in figure 24, and both of these envelopes will be used for the analysis of spoil pile stability.

Strength of jointed rock masses

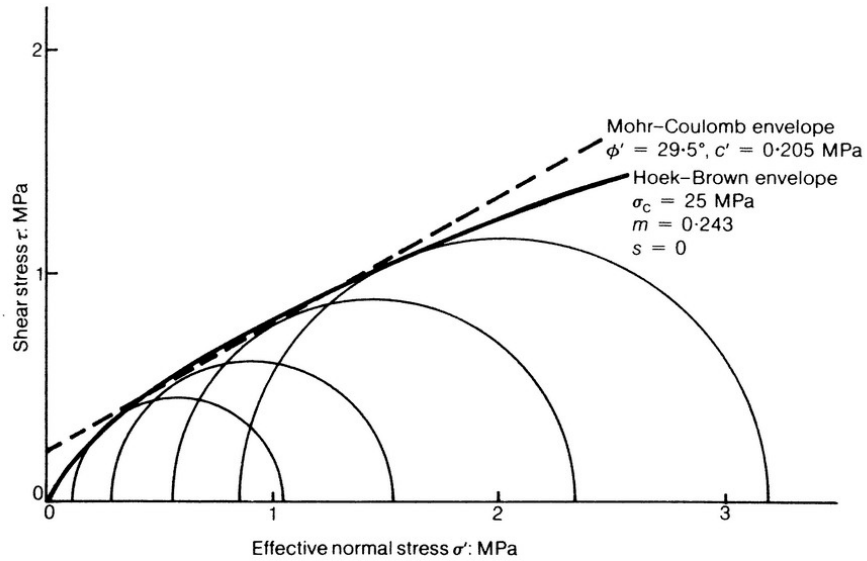


Figure 24 : Mohr circles derived from drained triaxial tests on retorted oil shale waste.

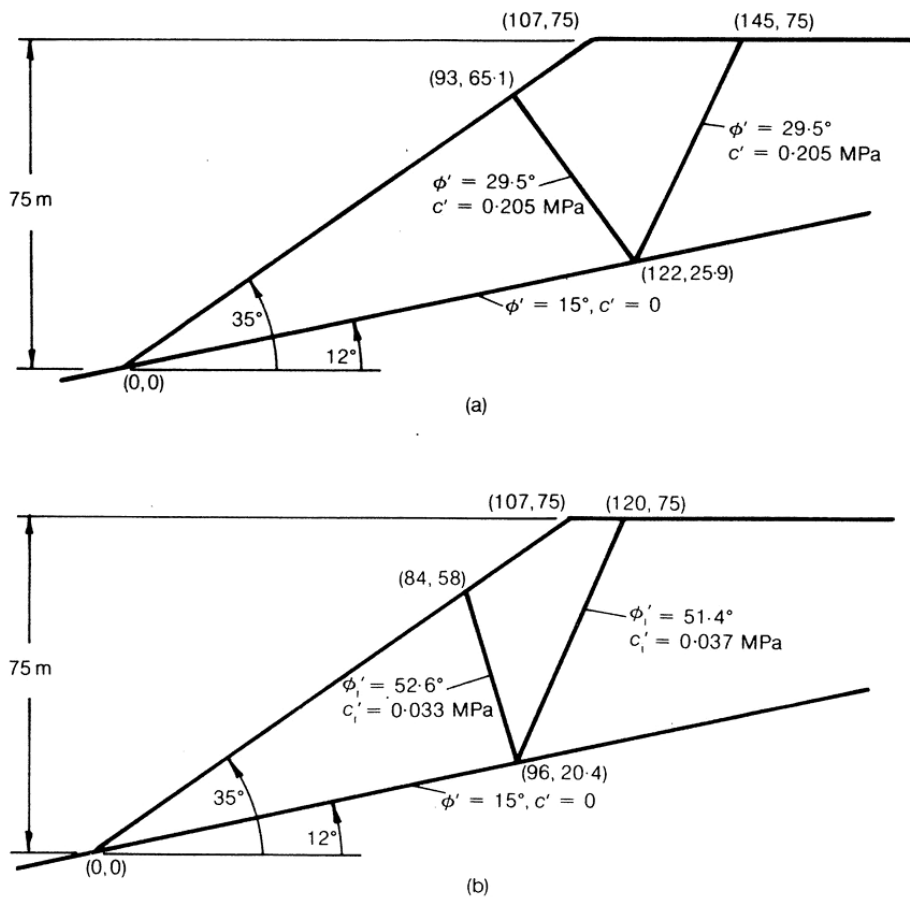


Figure 25 : Analyses of active-passive wedge failure in waste dumps of retorted oil shale resting on weak foundations. (a) Mohr-Coulomb failure criterion, factor of safety = 1.41; (b) Hoek-Brown failure criterion, factor of safety = 1.08

Figure 25 gives the results of stability analyses for the Mohr-Coulomb and Hoek-Brown failure criteria. These analyses were carried out by optimizing the angle of the interface between the active and passive wedge, followed by the angle of the back scarp followed by the distance of the back scarp behind the crest of the spoil pile. In each case, the angles and distances were varied to find the minimum factor of safety in accordance with the procedure suggested by Sarma (1979).

The factor of safety obtained for the Mohr-Coulomb failure criterion ($\phi' = 29.5^\circ$ and $c' = 0.205$) was 1.41, while that obtained for the Hoek-Brown criterion ($\sigma_c = 25$ MPa, $m = 0.243$ and $s = 0$) was 1.08. In studies on the reason for the difference between these two factors of safety, it was found that the normal stresses acting across the interface between the active and passive wedges and on the surface forming the back scarp range from 0.06 to 0.11 MPa. As can be seen from figure 24, this is the normal stress range in which no test data exists and where the linear Mohr-Coulomb failure envelope, fitted to test data at higher normal stress levels, tends to overestimate the available shear strength.

This example illustrates the importance of carrying out triaxial or direct shear tests at the effective normal stress levels which occur in the actual problem being studied. In the example considered here, it would have been more appropriate to carry out a preliminary stability analysis, based upon assumed parameters, before the testing programme was initiated. In this way, the correct range of normal stresses could have been used in the test. Unfortunately, as frequently happens in the real engineering world, limits of time, budget and available equipment means that it is not always possible to achieve the ideal testing and design sequence.

Conclusion

An empirical failure criterion for estimating the strength of jointed rock masses has been presented. The basis for its derivation, the assumptions made in its development, and its advantages and limitations have all been discussed. Three examples have been given to illustrate the application of this failure criterion in practical geotechnical engineering design.

From this discussion and from some of the questions left unanswered in the examples, it will be evident that a great deal more work remains to be done in this field. A better understanding of the mechanics of jointed rock mass behaviour is a problem of major significance in geotechnical engineering, and it is an understanding to which both the traditional disciplines of soil mechanics and rock mechanics can and must contribute. The author hopes that the ideas presented will contribute towards this understanding and development.

Acknowledgements

The author wishes to acknowledge the encouragement, assistance and guidance provided over many years by Professor E.T. Brown and Dr J.W. Bray of Imperial College. Many of the ideas presented originated from discussions with these colleagues and co-authors.

The simulating and challenging technical environment which is unique to the group of people who make up Golder Associates is also warmly acknowledged. This environment has provided the impetus and encouragement required by this author in searching for realistic solutions to practical engineering problems.

Particular thanks are due to Dr R. Hammett, Dr S. Dunbar, Mr M. Adler, Mr B. Stewart, Miss D. Mazurkewich and Miss S. Kerber for their assistance in the preparation of this paper.

Appendix 1 - Determination of material constants for empirical failure criterion.

Failure criterion

The failure criterion defined by equation 3

$$\sigma_1' = \sigma_3' + (m\sigma_c\sigma_3' + s\sigma_c^2)^{1/2} \quad (3)$$

can be rewritten as

$$y = m\sigma_c x + s\sigma_c^2 \quad (16)$$

where $y = (\sigma_1' - \sigma_3')^2$ and $x = \sigma_3'$

Intact rock

For intact rock, $s = 1$ and the uniaxial compressive strength σ_c and the material constant m are given by:

$$\sigma_c^2 = \frac{\sum y}{n} - \left[\frac{\sum xy - \frac{\sum x \sum y}{n}}{\sum x^2 - \frac{(\sum x)^2}{n}} \right] \frac{\sum x}{n} \quad (17)$$

$$m = \frac{1}{\sigma_c} \left[\frac{\sum xy - \frac{\sum x \sum y}{n}}{\sum x^2 - \frac{(\sum x)^2}{n}} \right] \quad (18)$$

where n is the number of data pairs.

The coefficient of determination r^2 is given by:

$$r^2 = \frac{(\sum xy - \sum x \sum y / n)^2}{(\sum x^2 - (\sum x)^2 / n)(\sum y^2 - (\sum y)^2 / n)} \quad (19)$$

Broken rock

For broken or heavily jointed rock, the strength of the intact rock pieces is determined by the analysis given above. The value of the constant m for broken or heavily jointed rock is found from equation 18. The value of the constant s is given by:

$$s = \frac{1}{\sigma_c^2} \left[\frac{\sum y}{n} - m \sigma_c \frac{\sum x}{n} \right] \quad (20)$$

The coefficient of determination is found from equation 19.

When the value of s is very close to zero, equation 20 will sometimes give a small negative value. In such cases, put $s = 0$ and calculate the constant m as follows:

$$m = \frac{\sum y}{\sigma_c \sum x} \quad (21)$$

Mohr envelope

The Mohr failure envelope is defined by the following equation, derived by Dr J.W. Bray of Imperial College:

$$\tau = (Cot \phi'_i - Cos \phi'_i) \frac{m \sigma_c}{8} \quad (22)$$

The value of the instantaneous friction angle ϕ'_i is given by:

$$\phi'_i = Arc \tan \left(4h \cos^2 (30 + 1/3 Arc \sin h^{-3/2}) - 1 \right)^{-1/2} \quad (23)$$

where

$$h = 1 + \frac{16 (m \sigma' + s \sigma_c)}{3m^2 \sigma_c}$$

and the instantaneous cohesive strength c'_i is given by:

$$c'_i = \tau - \sigma' \tan \phi'_i \quad (24)$$

where σ' is the effective normal stress.

Determination of m and s from direct shear test data

The following method for determination of the material constants m and s from direct shear test data was derived by Dr S. Dunbar (unpublished report) of Golder Associates in Vancouver.

The major and minor principal stresses σ'_1 and σ'_3 corresponding to each τ, σ' pair can be calculated as follows:

$$\sigma'_1 = \frac{(\sigma'^2 + (\tau - c')\tau) + \tau(\sigma'^2 + (\tau - c')^2)^{1/2}}{\sigma'} \quad (25)$$

$$\sigma'_3 = \frac{(\sigma'^2 + (\tau - c')\tau) - \tau(\sigma'^2 + (\tau - c')^2)^{1/2}}{\sigma'} \quad (26)$$

where c' is an estimate of the cohesion intercept for the entire τ, σ' data set. This value can be an assumed value greater than or equal to zero or it can be determined by linear regression analysis of the shear test results.

After calculation of the values of σ'_1 and σ'_3 by means of equations 25 and 26, the determination of the material constants m and s is carried out as for broken rock.

An estimate of the uniaxial compressive strength σ_c is required in order to complete the analysis.

References

- Barton, N.R. (1971). A relationship between joint roughness and joint shear strength. *Proc. Intl. Symp. Rock Fracture. Nancy, France*, paper No. 1-8.
- Barton, N.R. (1973). Review of a new shear strength criterion for rock joints. *Engineering Geol.* Vol. 7, 287-332.
- Barton, N.R. (1974). A review of the shear strength of filled discontinuities in rock. *Norwegian Geotech. Inst. Publ. No. 105.* Oslo: Norwegian Geotechnical Institute.
- Barton, N.R., Lien, R. and Lunde, J. (1974). Engineering classification of rock masses for the design of tunnel support. *Rock Mechanics.* Vol. 6, No. 4, 189-236.
- Barton, N.R. and Choubey, V. (1977). The shear strength of rock joints in theory and practice. *Rock Mechanics.* Vol. 10, No. 1-2, 1-54.
- Bieniawski, Z.T. (1974). Estimating the strength of rock materials. *J. South African Inst. Min. Metall.*, Vol. 74, No. 8, 312-320.
- Bieniawski, Z.T. (1974). Geomechanics classification of rock masses and its application in tunnelling. *Proc. 3rd Intl. Congr. Soc. Rock Mech.* Denver, 2, Part A, 27-32.
- Bieniawski, Z.T. (1976). Rock mass classification in rock engineering. In *Exploration for rock engineering : proceedings of the symposium*, Johannesburg, 1976, A.A. Balkema, Vol. 1, 97-106.
- Bishop, A.W., Webb, D.L. and Lewin, P.I. (1965). Undisturbed samples of London clay from the Ashford Common shaft. *Geotechnique*, Vol. 15, No. 1, 1-31.
- Bishop, A.W., and Garga, V.K. (1969). Drained tension tests on London clay. *Geotechnique*, Vol. 19, No. 2, 309-313.
- Brace, W.F. (1964). Brittle fracture of rocks. In *State of Stress in the Earth's Crust.* (ed. W.R. Judd) 111-174. New York: Elsevier.
- Brace, W.F. and Martin, R.J. (1968). A test of the law of effective stress for crystalline rocks of low porosity. *Intl. J. Rock Mech. Min. Sci.*, Vol. 5, No. 5,

- 415-426.
- Broch, E. (1974). The influence of water on some rock properties. *Proc. 3rd Congr. Intl. Soc. Rock Mech.* Denver, 2, Part A, 33-38.
- Brown, E.T. (1970). Strength of models of rock with intermittent joints. *J. Soil Mech. Found. Div., ASCE*, Vol. 96, SM6, 1935-1949.
- Brown, E.T. and Trollope, D.H. (1970). Strength of a model of jointed rock. *J. Soil Mech. Found. Div., ASCE*, Vol. 96, SM2, 685-704.
- Charles, J.A. and Watts, K.S. (1980). The influence of confining pressure on the shear strength of compacted rockfill. *Geotechnique*. Vol. 30, No. 4, 353-367.
- Colback, P.S.B. and Wiid, B.L. (1965). The influence of moisture content on the compressive strength of rock. *Proc. 3rd Canadian Rock Mechanics Symp.*, Toronto, 57-61.
- Coulthard, M.A. (1979). Back analysis of observed spoil failures using a two-wedge method. *Australian CSIRO Division of Applied Geomechanics*. Technical report, No. 83, Melbourne: CSIRO.
- Einstein, H.H., Nelson, R.A., Bruhn, R.W. and Hirschfeld, R.C. (1969). Model studies of jointed rock behaviour. *Proc. 11th Symp. Rock Mech.*, Berkeley, Calif., 83-103.
- Franklin, J.A. and Hoek, E. (1970). Developments in triaxial testing equipment. *Rock Mechanics*. Vol. 2, 223-228.
- Gerogiannopoulos, N.G.A. (1979). A critical state approach to rock mechanics. *PhD thesis*. Univ. London (Imperial College).
- Goodman, R.E. (1970). The deformability of joints. In *Determination of the in-situ modulus of deformation of rock*. ASTM Special Tech. Publ. No. 477, 174-196. Philadelphia: American Society for Testing and Materials.
- Griffith, A.A. (1921). The phenomena of rupture and flow in solids. *Phil. Trans. Royal Soc. (London) A*, Vol. 221, 163-198.
- Griffith, A.A. (1925). Theory of rupture. *Proc. 1st Congr. Appl. Mech.*, Delft, 1924. Delft: Technische Boekhandel en Drukkerij, 55-63.
- Handin, J., Hager, R.V., Friedman, M. and Feather, J.N. (1963). Experimental deformation of sedimentary rocks under confining pressure; pore pressure tests. *Bull. Amer. Assoc. Petrol. Geol.* Vol. 47, 717-755.
- Heard, H.C., Abey, A.E., Bonner, B.P. and Schock, R.N. (1974). Mechanical behaviour of dry Westerly granite at high confining pressure. *UCRL Report*, 51642. California: Lawrence Livermore Laboratory.
- Hencher, S.R. and Richards, L.R. (1982). The basic frictional resistance of sheeting joints in Hong Kong granite. *Hong Kong Engineer*. Feb., 21-25.
- Hobbs, D.W. (1970). The behaviour of broken rock under triaxial compression. *Intl. J. Rock Mech. Min. Sci.* Vol. 7, 125-148.
- Hoek, E. (1964). Fracture of anisotropic rock. *J. South African Inst. Min. Metall.* Vol. 64, No. 10, 510-518.
- Hoek, E. (1965). Rock fracture under static stress conditions. *PhD Thesis*, Univ. Cape Town.
- Hoek, E. (1968). Brittle failure of rock. In *Rock Mechanics in Engineering Practice*. (eds K.G. Stagg and O.C. Zienkiewicz) London: Wiley. 99-124.
- Hoek, E. and Bieniawski, Z.T. (1965). Brittle fracture propagation in rock under compression. *Intl. J. Fracture Mechanics*. Vol. 1, No. 3, 137-155.
- Hoek, E. and Brown, E.T. (1980a). *Underground Excavations in Rock*. London: Inst. Min. Metall.
- Hoek, E. and Brown, E.T. (1980b). Empirical strength criterion for rock masses. *J.*

- Geotech. Engin. Div., ASCE*, Vol. 106, No. GT9, 1013-1035.
- Hoek, E. and Bray, J.W. (1981). *Rock Slope Engineering*. (Third ed.) London: Inst. Min. Metall.
- Hoek, E. General two-dimensional slope stability analysis. In *Analytical and Numerical Methods in Rock Engineering* (ed. E.T. Brown). London: Geo. Allen & Unwin. in press.
- Horino, F.G. and Ellikson, M.L. (1970). A method of estimating the strength of rock containing planes of weakness. *U.S. Bur. Mines Rept. Invest.* 7449.
- Horn, H.M. and Hendron, D.M. (1968). Discussion on 'Stability analysis for a sloping core embankment'. *J. Soil Mech. Found. Div., ASCE*, Vol. 94, SM3, 777-779.
- Jaeger, J.C. (1970). The behaviour of closely jointed rock. *Proc. 11th Symp. Rock Mech.*, Berkeley, California, 57-68.
- Jaeger, J.C. (1971). Friction of rocks and stability of rock slopes. *Geotechnique*, Vol. 21, No. 2, 97-134.
- Jaeger, J.C. and Cook, N.G.W. (1969). *Fundamentals of Rock Mechanics*. London: Chapman and Hall.
- John, K.W. (1962). An approach to rock mechanics. *J. Soil Mech. Found. Div., ASCE*, Vol. 88, SM4, 1-30.
- Krsmanovic, D. (1967). Initial and residual shear strength of hard rock. *Geotechnique*. Vol. 17, No. 2, 145-160.
- Ladanyi, B. and Archambault, G. (1970). Simulation of shear behaviour of a jointed rock mass. *Proc. 11th Symp. Rock Mech.*, 105-125. New York: American Institute of Mining, Metallurgical and Petroleum Engineers.
- Ladanyi, B. and Archambault, G. (1972). Evaluation de la resistance au cisaillement d'un massif rocheux fragmente. *Proc. 24th Intl. Geol. Cong.*, Montreal. Sect. 130, 249-260.
- Lajtai, E.Z. (1967). The influence of interlocking rock discontinuities on compressive strength (model experiments). *Rock Mech. Eng. Geol.* Vol. 5, 217-228.
- Lama, R.C. and Vutukuri, V.S. (1978). *Handbook on Mechanical Properties of Rocks. Vol.IV - Testing Techniques and Results*. Switzerland: Trans Tech Publications.
- Marachi, N.D., Chan, C.K. and Seed, H.B. (1972). Evaluation of properties of rockfill materials. *J. Soil Mechs. Fdns. Div. ASCE*, Vol. 98, SM4, 95-114.
- Marsal, R.J. (1967). Large scale testing of rockfill materials. *J. Soil Mech. Fdns. Div. ASCE*, Vol. 93, SM2, 27-44.
- Marsal, R.J. (1973). Mechanical properties of rockfill. *Embankment Dam Engineering, Casagrande Vol.*, 109-200. New York: Wiley.
- Martin, G.R. and Miller, (1974). Joint strength characteristics of a weathered rock. *Proc. 3rd Cong. Intl. Soc. Rock Mech.*, Denver. Vol. 2, Part A, 263-270.
- McClintock, F.A. and Walsh, J.B. (1967). Friction on Griffith cracks under pressure. *Proc. 4th U.S. Congr. Appl. Math.*, Berkeley. 1015-1021.
- McLamore, R. and Gray, K.E. (1967). The mechanical behaviour of anisotropic sedimentary rocks. *Trans. Am. Soc. Mech. Engrs. Series B*, 62-76.
- Misra, B. (1972). Correlation of rock properties with machine performance. *PhD. Thesis*, Leeds University.
- Mogi, K. (1966). Pressure dependence of rock strength and transition from brittle fracture to ductile flow. *Bull. Earthquake Res. Inst. Tokyo University*, Vol. 44, 215-232.
- Mogi, K. (1967). Effect of the intermediate principal stress on rock failure. *J. Geophys. Res.*, Vol. 72, No. 20, 5117-5131.

- Muller, L. and Pacher, F. (1965). Modelevensuch Zur Klarung der Bruchgefahr geklufteter Medien. *Rock Mech. Engng Geol. Supp.* No.2, 7-24.
- Murrell, S.A.F. (1958). The strength of coal under triaxial compression. In *Mechanical properties of non-metallic brittle materials.* (ed. W.H. Walton), 123-145. London: Butterworths.
- Murrell, S.A.F. (1965). The effect of triaxial stress systems on the strength of rocks at atmospheric temperatures. *Geophysics J.*, Vol. 10, 231-281.
- Patton, F.D. (1966). Multiple modes of shear failure in rock. *Proc. Inst. Intl. Cong. Rock Mech.*, Lisbon, Vol. 1, 509-513.
- Raphael, J.M. and Goodman, R.E. (1979). Strength of deformability of highly fractured rock. *J. Geotech. Eng. Div., ASCE*, Vol. 105, GT11, 1285-1300.
- Richards, L.R. and Cowland, J.W. (1982). The effect of surface roughness on field shear strength of sheeting joints in Hong Kong granite. *Hong Kong Engineer*, Oct., 39-43.
- Rosengren, K.J. and Jaeger, J.C. (1968). The mechanical properties of a low-porosity interlocked aggregate. *Geotechnique*. Vol. 18, No.3, 317-326.
- Sarma, S.K. (1979). Stability analysis of embankments and slopes. *J. Geotech. Eng. Div., ASCE*, Vol. 105, GT12, 1511-1524.
- Schwartz, A.E. (1964). Failure of rock in the triaxial shear test. *Proc. 6th Rock Mech. Symp.* Rolla, Missouri, 109-135.
- Seed, H.B. and Sultan, H.A. (1967). Stability analysis for sloping core embankment. *J. Geotech. Eng. Div., ASCE*, Vol. 93, SM4, 69 -83.
- Walker, P.E. (1971). The shearing behaviour of a block jointed rock model. *PhD Thesis*, Queens Univ. Belfast.
- Wawersik, W.R. (1969). Detailed analysis of rock failure in laboratory compression tests. *PhD Thesis*, Univ. of Minnesota.
- Wawersik, W.R. and Brace, W.F. (1971). Post failure behaviour of a granite and a diabase. *Rock Mechanics*. Vol. 3, No. 2, 61-85.